

Permafrost detection using cryotic assessment sites in Nain, Nunatsiavut

by

Jesse Korn 20344589

Supervisor: Dr. Robert Way

Examiner: Dr. Christian Seiler

04/17/2025

## Abstract

Permafrost environments are warming in the face of climate change, with impacts on infrastructure and development in the North. The community of Nain, Nunatsiavut (Labrador) requires rapid infrastructure development to support its growing population and to address deteriorating existing infrastructure. Nain is located in the sporadic discontinuous permafrost zone, and future development areas may be underlain by permafrost. Due to climate change and anthropogenic activities, permafrost in Nain has been thawing, leading to ground subsidence and infrastructure damage in portions of the community. There is now a clear need for improved assessment of permafrost distribution in Nain to support climate-resilient development and planning.

Here we present the results of field investigations of permafrost distribution in Nain using data collected in Summer 2025 from 84 Cryotic Assessment Sites (CAS). At each location, instantaneous ground temperature profiles were measured with a cryotic assessment temperature probe (CAT probe), and site conditions were characterized *in situ*. This allowed for estimation of the presence or absence of cryotic ground up to a depth of 3.5 m. We found that 39% of the CAS (33/84) were predicted or confirmed to be underlain by cryotic ground, with most of these locations found in undeveloped parts of the community. Notably, cryotic ground was inferred to be widespread on a steep south-facing slope above community housing and in a prime development area near the community airstrip, which may present development challenges. This project is a part of a larger effort to map geocryological hazards across Nain for the Nunatsiavut Government and the Nain Inuit Community Government.

## **Statement of Originality and Disclosure of Use of Artificial Intelligence**

Generative AI was not used to write any part of this undergraduate thesis. Generative AI was used to assist with coding in R with permission from a supervisor. This includes assisting in repetitive code to run large amounts of extrapolations, asking general coding questions, and generating code used for organizing graphing. Outputs were also compared with manual extrapolations done in Excel to ensure accuracy in the partially AI generated R code.

## **Acknowledgments**

I would like to acknowledge that the data presented in this thesis was collected on Labrador Inuit Lands. This research was undertaken in accordance with a permit issued by the Nunatsiavut Government's Research Advisory Committee (permit no: NGRAC-68175979).

Firstly I would like to thank my wonderful supervisor Dr. Robert Way for his thoughtful guidance throughout this project. Thank you to Madison Power, Rachel Tian, and Dr. Yifeng Wang for assisting with data collection and supporting this project. Thank you to the Nunatsiavut Government, the Nunatsiavut Research Centre, and the Nain Inuit Community Government for supporting permafrost research in Nunatsiavut and Nain specifically. I also want to thank my Father David, and friends Bryan, and Kenny for proof reading this thesis and Anandi for supporting me throughout the whole season.

## Table of contents

Title page.....	1
Abstract.....	2
Statement of Originality and Disclosure of Use of Artificial Intelligence.....	3
Acknowledgements.....	3
Table of contents.....	4
List of figures.....	6
List of equations.....	7
List of tables.....	7
List of abbreviations.....	8
Chapter 1: Introduction.....	9
1.1 Background.....	9
1.2 Research goal.....	10
1.3 Expected significance.....	11
Chapter 2: Literature review.....	12
2.1 Permafrost, the active layer, and geohazards.....	12
2.2 Permafrost detection and mapping.....	13
2.3 Factors influencing permafrost distribution.....	14
Chapter 3: Methods.....	16
3.1 Study area.....	16
3.2 Data collection with CAT probes.....	17
3.3 Other field measurements.....	19
3.4 Field sampling design.....	20
3.5 Extrapolation of CAT probe measurements.....	21
3.6 Determining local site influences on cryotic ground distribution.....	25

Chapter 4: Results.....	27
4.1 Measured ground temperatures & evaluation of extrapolation methods..	27
4.2 Cryotic assessment site results for Nain.....	30
4.3 Assessing variable correlation.....	32
4.2a Random forest for observed variables.....	32
4.2b Random forest for vegetation.....	37
Chapter 5: Discussion.....	39
5.1 Ground temperature measurements and regression results.....	39
5.2 Influence of local site characteristics on CAS results.....	40
5.3 Permafrost in the community of Nain, Nunatsiavut.....	43
5.4 Limitations and improvements.....	45
5.5 Future work.....	47
Chapter 6: Conclusion.....	47
References.....	48
Appendix A: Supplemental materials.....	51
A1 Table of CAT probe measurements with ALT results.....	51
A2 Variable partial dependence plot.....	54
A3 Vegetation partial dependence plot.....	55
A4 Sheet used to document CAS information in the field.....	56
A5 Descriptions of how variables were collected in the field.....	58
A6 All CAS temperature points.....	60
A7 All CAS variables.....	66

## List of figures

**Figure 2.1:** Map depicting the study area of Nain ( $56^{\circ}32'N$ ,  $61^{\circ}42'W$ ) at scale of the eastern provinces.

**Figure 3.1:** Diagram depicting a cross section profile of a CAT probe underground.

**Figure 3.2.** A) CAT probe in the ground; B) CAT probe and HOBO loggers in tupperware containers; C) Digging soil pit so frost probe can reach target depths.

**Figure 3.3.** Map of the completed cryotic assessment sites in Nain ( $56^{\circ}32'N$ ,  $61^{\circ}42'W$ ), 84 in total. Inset map marks Nain's location in Canada.

**Figure 3.4.** Nain ( $56^{\circ}32'N$ ,  $61^{\circ}42'W$ ) Surficial Materials map with completed CAS points overlain. Surficial material data from Bell (2011). Inset map marks Nain's location in Canada.

**Figure 3.5:** Ensemble of 240 simulated daily ground temperature profiles for August 15, 2025 from Colyn et al. (2025).

**Figure 3.6:** Visualization of all extrapolation types applied to CAS 32. See appendix A6 for details on CAS 32.

**Figure 4.1:** Results of all CAT probe readings in a graph with a power series trendline.

**Figure 4.2.** Map of CAS points and their predicted permafrost presence using ALT (see table 4.2).

**Figure 4.4:** Graph of mean decrease accuracy of the first run of the forest model on observed variables.

**Table 4.4:** Table depicting the output of the random forest model as a confusion matrix.

**Table 4.3:** Table of results using the prediction model developed from the random forest model.

**Figure 4.5:** Graph of the mean decrease accuracy for variables (excluding plant types, snow cover, soil texture, canopy cover, and organic layer thickness)

**Figure 4.6.** A series of plots depicting the partial dependence of the prediction of cryotic ground absence based on various variables.

**Figure 4.7:** Figure 4.6a with the dependent variable changed to *present*.

**Figure 4.8:** Graph of the mean decrease accuracy for vegetation types.

**Figure 4.3.** Map of CAS points and the predicted depth of the active layer using LOESS.

**Figure 5.1:** Map of cryotic ground presence divided into sections.

**Figure 5.2:**

### List of equations

**Equation 3.1.** Eq. (27) from Uxa et al. (2026).

### List of tables

**Table 4.1:** Results of extrapolation method comparison using simulated temperatures from Colyn (2024).

**Table 4.2.** Table of ALT extrapolations of CAS points with a cutoff of 300cm.

**Table 4.3:** Table depicting the output of the random forest model as a confusion matrix.

**Table 4.4:** Table depicting the output of the random forest model as a confusion matrix for vegetation types.

## List of abbreviations

ALT: Active Layer Thickness

a.s.l: above sea level

BTS: Basal Temperature of Snow

CAS: Cryotic Assessment Site

CAT: Cryotic Assessment Temperature

DC: Direct Current

ERT: Electrical Resistivity Tomography

LOESS: Locally Estimated Scatterplot Smoothing

## Chapter 1: Introduction

### 1.1 Background

Permafrost is perennially cryotic ground, and is therefore at or below 0°C for 2 years or more (French and Slaymaker 2012). The area above permafrost is subject to seasonal freeze and thaw cycles called the active layer. Changes to climate and anthropogenic activities can change the local surface energy balance, leading to permafrost thaw and thickening of the active layer (French and Slaymaker 2012). Thawing permafrost can result in ground ice melt, which has the potential to cause ground subsidence and structural damage to infrastructure overlaying permafrost (GRID-Arendal 2020, Way et al. 2021). Historically, permafrost research in Canada has been predominantly focused on the western Subarctic or High Arctic regions, whereas northeastern Canada and Nunatsiavut specifically is understudied (Power et al. 2025).

The community of Nain, Nunatsiavut, is located in the sporadic discontinuous permafrost zone and has experienced subsidence within the town from permafrost thaw (Way et al. 2021). Detecting and mapping permafrost across the community has been identified as a priority by the Nunatsiavut Government to support planning and infrastructure development (*Silavut Asianguvalliujuk Nunatsiavut Climate Change Workshop* 2024). Previous research on permafrost in Nain has focused on locations of existing infrastructure (Way et al. 2021), but greater knowledge about permafrost around the community is needed. This BSc project aims to contribute to this knowledge base through assessing the presence of permafrost at cryotic assessment sites throughout the community.

This research is a contribution to a much larger project entitled ‘Snow, Ice & Soil: Adaptation to a changing cryosphere in Nunatsiavut’ (SISAdapt). In 2025, in collaboration with the Nunatsiavut Government, the Northern Environmental Geoscience Laboratory launched the SISAdapt Project. This thesis contributes to SISAdapt’s Soil theme and supports the overarching SISAdapt project objective of geohazard mapping. Correspondingly, the locations of the specific investigations described in this thesis were determined in collaboration with other research team members, the Nunatsiavut Government, and its partners to produce new information about permafrost in potential development areas within the boundaries of Nain using a variety of research methods.

## **1.2 Research goal**

The goal of this research is to assess permafrost absence or presence at Cryotic Assessment Sites (CAS) collected in Summer 2025 throughout Nain and to understand the local-scale factors influencing permafrost distribution in the region. This will be accomplished through the following objectives:

1. Determination of cryotic ground presence or absence at 84 locations in Nain using ground temperature gradients measured *in situ*.
2. Evaluation of the influences of local ecosystem and landscape factors on cryotic ground distribution in Nain.

### ***1.3 Expected significance***

This research will support ongoing geohazard mapping in the remote Inuit community of Nain, Nunatsiavut. Nain requires rapid infrastructure growth to support its increasing population. However, permafrost thaw threatens the longevity and safety of infrastructure underlain by permafrost due to an increased risk of geohazards, such as landslides (Patton et al. 2021). Mapping permafrost beforehand can help planners make informed decisions for construction projects. Permafrost evaluation on the hill over the community will also inform whether thaw-related landslides are a potential risk to existing community infrastructure. Cryotic assessment site data from this thesis will also aid in ground truthing of other mapping techniques used in Nain for the SISAdapt project.

## Chapter 2: Literature review

### ***2.1 Permafrost, the active layer, and geohazards***

Permafrost is soil and or rock that remains below 0°C for 2 consecutive years (French and Slaymaker 2012). Permafrost is not necessarily frozen, as the freezing point of water can be modified by factors such as pressure and salinity (French and Slaymaker 2012). The presence of moisture or ice is also not a requirement. Therefore, permafrost is defined by whether it is cryotic (<0°C ) or non-cryotic (>0°C). Above permafrost is the active layer which seasonally thaws each summer and refreezes each winter. Usually seasonal freezing of the active layer reaches the permafrost table. However, there can be an unfrozen zone between permafrost and the active layer called a supra-permafrost talik (French and Slaymaker 2012). The thaw of permafrost can lead to geohazards, which pose a threat to infrastructure, the environment, and people.

Warming climate and anthropogenic activities can thaw permafrost, increasing ground temperatures and active layer thickness. The thaw of permafrost has been shown to cause thaw related ground subsidence which can damage the integrity of structures overlaying them (Fortier and Bolduc 2008). Permafrost thaw can also mobilize contaminants stored within it, contributing to climate warming processes and contaminating the environment. Thaw can also result in the loss of hydrological barriers, soil instability, and increased hydrological connectivity (Langer et al. 2023). These factors can aid in the formation of a landslide or related landforms, which has the potential to be extremely hazardous (Patton et al. 2021).

## ***2.2 Permafrost detection and mapping***

Detecting or predicting permafrost in the field can be done using direct methods or indirect methods. Direct methods utilize physical measurements within the subsurface in order to measure permafrost presence. Indirect methods use remote techniques to map indicators which generate predictions of where permafrost would be. Indirect mapping can be further reinforced with “ground truthing” from direct methods, such as when direct methods are used to verify the conclusions of indirect mapping.

Direct detection of near-surface permafrost is most commonly performed with a frost probe, a metal T-shaped pole typically 100 to 120 cm long. The frost probe is inserted into the soil until it reaches a depth of refusal or until the maximum length of the probe is reached (Boike et al. 2022). At the point of refusal, the presence can be determined through the distinctive sound and feeling of ice contact. Frost probing accuracy may vary based on the strength and size of the operator, leading to potential error or bias (Smith et al. 2009). Furthermore, frost probing does not account for cryotic but unfrozen regions in ice-rich permafrost and can inaccurately depict active layer depths (Streletskiy et al. 2017).

Studies have proposed using ground temperature measurements to directly detect the absence or presence of permafrost to circumvent issues with frost probing (Bonnaventure and Lewkowicz 2008, Way et al. 2021, Daly et al. 2022, Nicholson 2025). These measurements are typically collected with a probe or pole that contains vertically arranged temperature sensors. The data from these sensors are then used to directly detect cryotic ground, if present, or are extrapolated to deeper depths, allowing for a prediction of the depth at which permafrost may be encountered (Daly

et al. 2022, Nicholson 2025). The accuracy of extrapolation is dependent on the number of measurements extrapolated from, where more measurements increase accuracy (Riseborough 2008).

Ground temperatures were utilized as a ground truthing method to understand permafrost absence or presence across an array of sites including locations of direct current (DC) electrical resistivity tomography (ERT) and basal temperature of snow (BTS) surveys completed for other components of SISAdapt. ERT utilizes electrical resistivity measurements to create a resistivity tomogram of the subsurface that can be used to characterize discontinuous permafrost (Herring et al. 2023). BTS, utilises temperatures from the bottom of the snowpack to predict ground temperatures and permafrost presence.

### ***2.3 Factors influencing permafrost distribution***

Permafrost presence can be influenced by a series of factors such as proximity to water bodies, exposure to the elements, and plant cover. These factors can be used to help predict or explain permafrost presence or absence. For example, water bodies modify the temperatures of surrounding areas (Hugh M. French and Olav Slaymaker 2012). This decreases the potential distribution of permafrost near shorelines, as waterbodies can warm ground temperatures. Snow cover from the winter months can influence summer ground temperatures. Snow has an insulating effect, and so ground with thicker snowpacks is insulated from cold winter temperatures, reducing the time for cooling to occur (Zhang 2005). This indicates that snowpack thickness will influence permafrost presence. Windswept

regions can have thinner and denser snowpacks, which can increase permafrost aggradation (Zhang 2005). Regions where this blown snow is deposited will have thicker snowpacks and therefore will reduce permafrost formation (Zhang 2005). These snowpack factors can interact with local vegetation. Trees can intercept snowfall causing snowpack to become shallower on the ground. Vegetation such as shrubs have the ability to shade the ground and trap snow increasing the depth of the snowpack. During summer, this shading cools the ground, reducing thaw, but in the winter, it has the ability to insulate the ground due to the increased snowpack (Heijmans et al. 2022).

Another factor that can interact with permafrost presence is soil moisture. Permafrost has been found to enhance surface water retention by impeding infiltration. This results in higher moisture content near the base of the active layer (Xiao et al. 2025). Furthermore some surficial material classes are more frost-susceptible. Fine grained materials such as silts and clays can readily form ice. The latent heat from which can mobilize water and result in complex thermal and physical conditions (Lafrenière and Lamoureux 2019). Thus permafrost presence can be subject to variability making it difficult to predict permafrost presence on these variables alone.

## Chapter 3: Methods

### 3.1 Study area

Field investigations took place in and around the community of Nain (56°32'N, 61°42'W), Nunatsiavut, NL, from July 25th to August 12th, 2025. Nain is the largest and northernmost community in Nunatsiavut and is only accessible by plane or boat in the summer months. Community infrastructure, including new housing subdivisions are urgently required to support the needs of the growing community. Nain has a subarctic climate, a mean annual air temperature of -2.5°C, an annual temperature range of 37.6°C. Total annual precipitation is 925.5 mm, 475.3 mm of which is snowfall. This data is from the Canadian climate normals 1981-2010 (Environment Canada 2025). Nain is located in an east-facing valley surrounded by hills reaching ~275 m a.s.l. The community is underlain by various surficial deposits, including marine, glaciomarine, glaciofluvial, glaciocolluvial, concealed bedrock / till, alluvial, and disturbed sediments (Bell 2011).

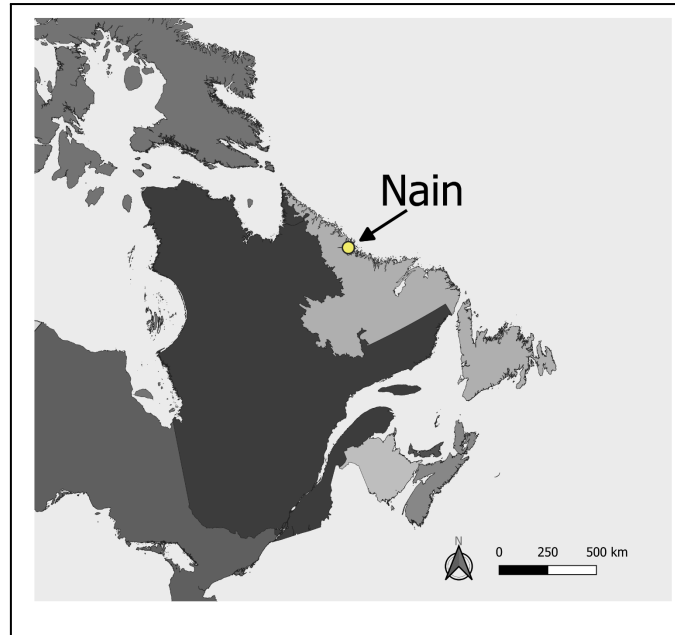


**Figure 2.1:** Map depicting the location of Nain ( $56^{\circ}32'N$ ,  $61^{\circ}42'W$ ) relative to Canada's eastern provinces.

### **3.2 Data collection with CAT probes**

Two cryotic assessment temperature (CAT) probes were assembled to measure ground temperature profiles at CAS points distributed across the community of Nain to the target depth of 150 cm (Figure 1, Figure 2A). Six thermistors (Onset TMCx-HD,  $\pm 0.15^{\circ}C$  with UX120) were attached to wooden dowels with electrical tape at 20 cm spacing spanning 20 cm - 120 cm of measurement. The six thermistors were attached to two 4-channel HOBO UX120-006M analog data loggers for each probe. The UX120-006M has a real-time temperature display and a margin of error of  $\pm 0.1^{\circ}C$  according to ice bath tests of thermistors and loggers conducted prior to fieldwork. This CAT probe is similar in its configuration to those used by Way & Lewkowicz (2015), Holloway and Lewkowicz (2020), Way et al (2021) and Daly et al (2022), amongst others. Ground temperatures were recorded 15 minutes after insertion so as to allow for thermal equilibration.

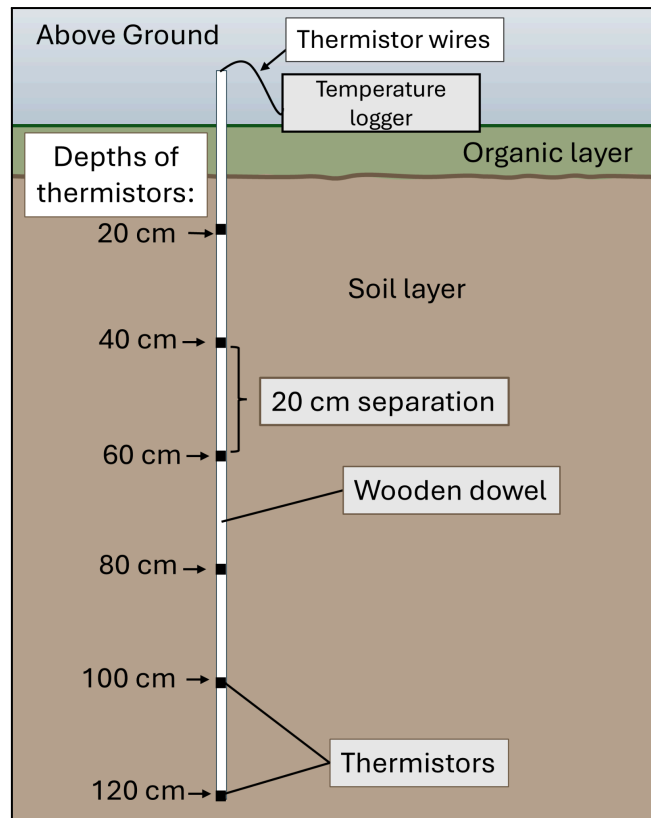


**Figure 3.1:** Diagram depicting a cross section profile of a CAT probe underground.

CAT probes were inserted into the ground to a target depth of 150 cm using holes created with a frost probe (122 cm length  $\frac{5}{8}$ " tile probe from AMS Inc.) and/or a handheld battery-powered hammer drill (RYOBI 18V ONE + Rotary Hammer) with an extended length bit of 90 cm. As the frost probe and drill bit were not long enough to reach the target depth of 150 cm, shallow soil pits were dug using a shovel prior to probing/drilling to allow the target depth to be reached (see Figure 3.2C).



**Figure 3.2:** A) CAT probe in the ground; B) CAT probe and HOBO loggers in waterproof containers; C) Digging soil pit so frost probe can reach target depths.

### **3.3 Other field measurements**

Organic layer thickness, maximum vegetation heights, percent cover of vegetation, canopy cover, soil moisture, soil texture, vegetation types, snow cover, drainage class, and slope were documented for each CAS following methods described by (Colyn et al. 2025). Soil moisture and texture types were determined using the *Ecosystems of the Yukon Arctic Region: A Guide to Identification* (MacKenzie et al. 2022). See appendix A4 and appendix A5 for collection details.

### **3.4 Field sampling design**

CAS locations were selected using surficial material strata defined using a local surficial materials map from the landscape hazard assessment in Nain (Bell et al. 2011). Originally, eight strata for CAS points were chosen: marine + glaciomarine, glacio-colluvial, glacio-fluvial, disturbed, concealed bedrock / till, alluvial, higher ground, and lower ground. Ten randomized points in each of these regions were generated with ArcGIS Pro 3.5.0, and at least five in each surficial type were selected as a CAS. Randomized CAS points located on community infrastructure (e.g. residential housing) and points located on inaccessible or unsafe terrain were excluded from evaluation. In these situations, a point nearby was selected instead. This could lead to points being up to ~100 m away from their original target location. Higher elevation and lower elevation CAS points were generated to compare elevation with permafrost presence, but for safety reasons the CAS points on steep slopes were not visited. The concealed bedrock with thin till class was also removed as our drill bit was unable to pierce most of the points in this strata (except one location). Concealed bedrock / till points are located at higher and more dangerous elevations, which also contributed to their exclusion. CAS points were also located along ERT lines and basal temperature of snow measurement locations to support the larger SISAdapt project.

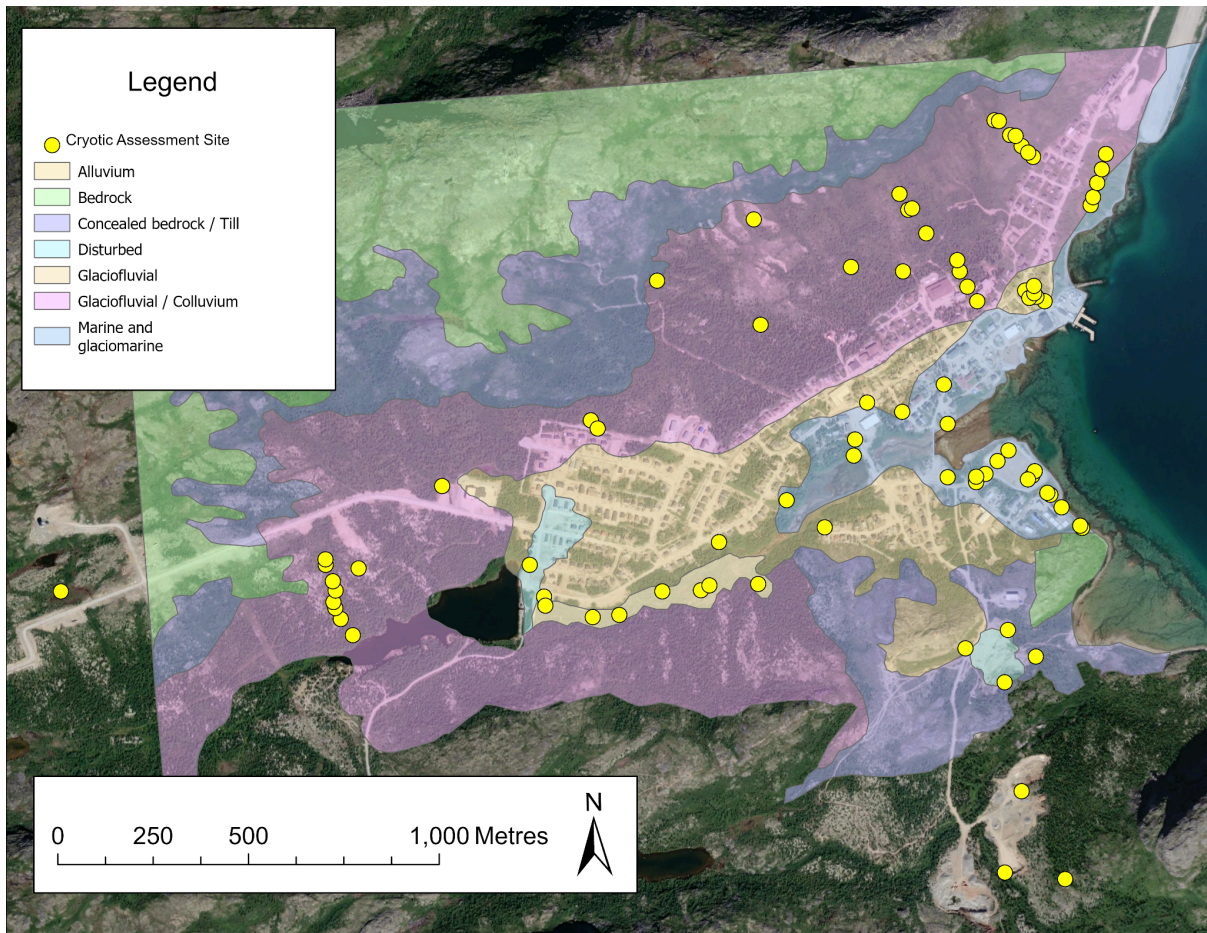


**Figure 3.4:** Nain (56°32' N, 61°42'W) Surficial Materials map with completed CAS points overlain. Surficial material data from Bell et al. (2011).

### 3.5 Extrapolation of CAT probe measurements

Permafrost presence or absence can be inferred through the extrapolation of ground temperature measurements. A variety of extrapolation approaches have been applied to ground temperature profiles collected *in situ* with linear extrapolations being the most common (Bonnaventure and Lewkowicz 2008, Daly et al. 2022, Nicholson 2025). However, the ground thermal regime is often non-linear with depth (Figure 4.1) therefore linear extrapolation may not best characterize the presence or absence of cryotic ground at depth. To evaluate different methods of extrapolation that could be applied to CAT probe data, ground thermal simulation

data from Colyn et al. (2025) was extrapolated utilizing a variety of methods to compare the accuracy of different methods (Figure 3.5). Simulation temperature data from depths of 25, 45, 65, 85, 108, and 123 cm were used to compare each extrapolation approach. These depths were chosen to mimic the intervals collected in the field (Appendix A6).

The simulation from Colyn et al. (2025) used a one dimensional surface energy balance model called the Northern Ecosystem Soil Temperature model (Zhang et al. 2003). This model has been previously successfully applied to permafrost environments in Labrador (Tutton et al. 2021, Wang and Way 2025). The simulation included data from four locations across Labrador (including the Nain area) and the daily mean ground temperatures used in the profiles were from August 15th, 2023 representing the middle of the thaw season.

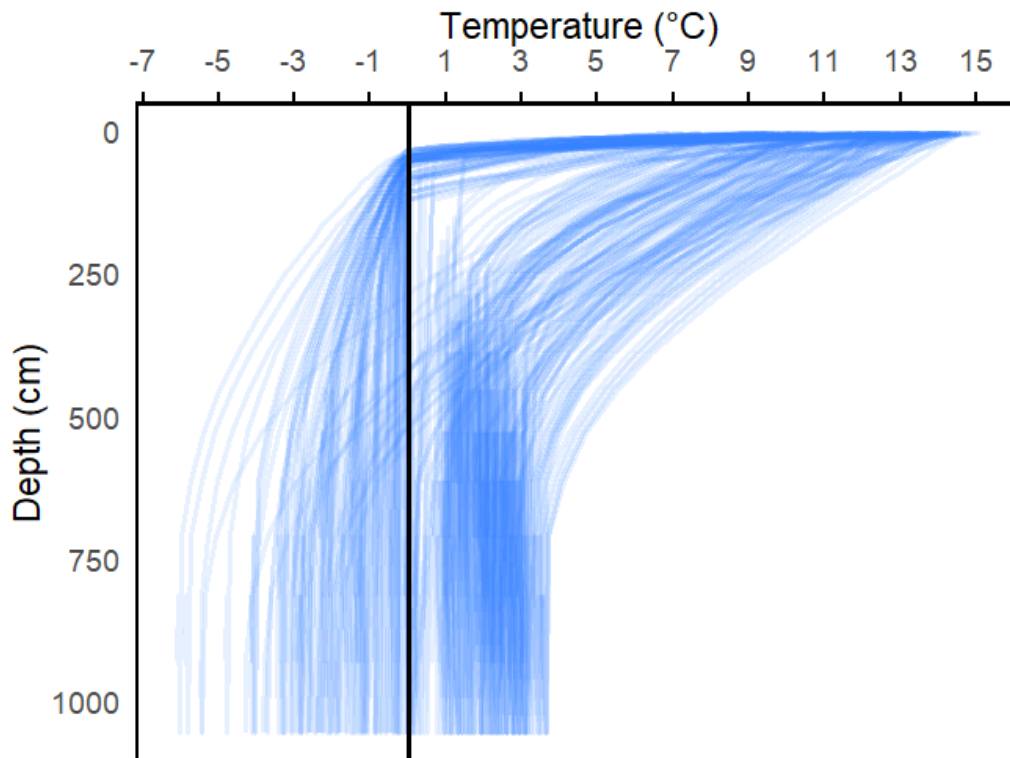


**Figure 3.5:** Ensemble of 240 simulated daily ground temperature profiles for August 15, 2025 from Colyn et al. (2025).

Two-hundred and forty simulated CAS were analysed with the eight extrapolation methods, resulting in 1920 extrapolated ground temperature profiles (Figure 3.6). Four of the extrapolation methods were linear regressions that consisted of using all six, the three deepest, the two deepest, and the deepest and shallowest temperature points. Non-linear extrapolation approaches included locally estimated scatterplot smoothing (LOESS) using all points, Active Layer Thickness (ALT) estimation from Uxa et al. (2026), and 2nd polynomial fits using all 6 and the 3 deepest temperature points. Figure 3.6 visualises all these extrapolations on a sample CAS point.

Eq. (27) from Uxa et al. (2026) was used to calculate the ALT. While this equation is written as  $l_{TZx}$  = thawing index at depth  $Z_x$ , the formula was modified for our purposes. Where  $Z_x$  = the depth of a point and  $l_{TZx}$  = the temperature at  $Z_x$ . The two deepest points that were above 0°C were used for this equation.

$$\text{ALT} = \frac{Z_2\sqrt{l_{TZ1}} - Z_1\sqrt{l_{TZ2}}}{\sqrt{l_{tZ1}} - \sqrt{l_{tZ2}}}$$

**Equation 3.1:** Eq. (27) from Uxa et al. (2026).

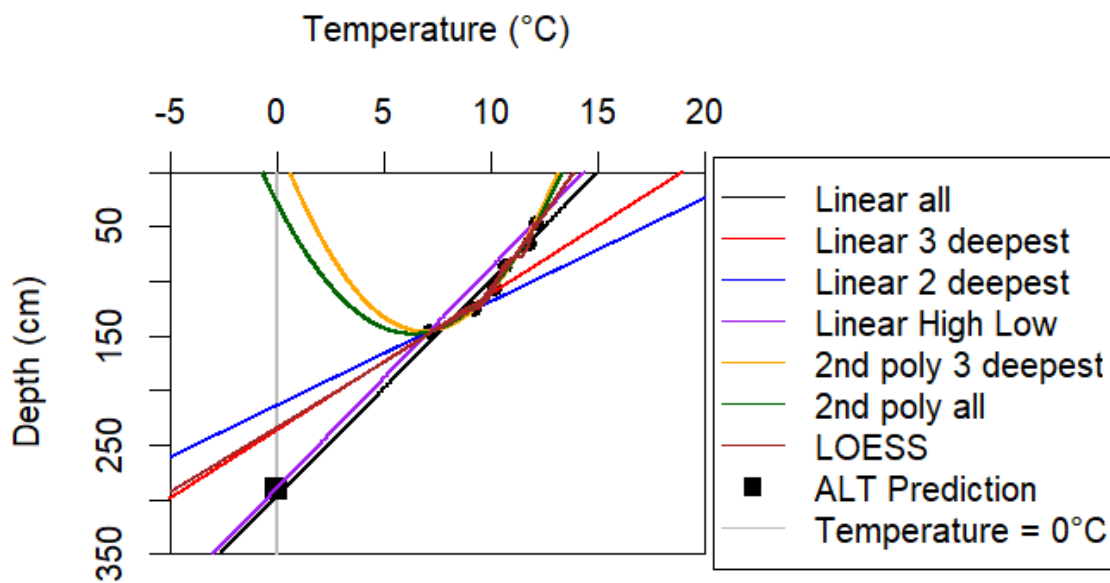


**Figure 3.6:** Visualization of all extrapolation types applied to CAS 32. See appendix A6 for details on CAS 32.

The maximum depth for extrapolation was set at 3.0 m due to an increase in extrapolation errors after that depth, though errors again increased notably below 3.5 m so we did apply methods to depths of 3.5 m as well for comparison but not below that depth. A confusion matrix was used to determine precision, accuracy, and

specificity for each extrapolation method. Precision displays the proportion of true positive predictions using the formula  $\text{True Positive} / (\text{True Positive} + \text{False Positive})$ . Accuracy is a ratio between correct and incorrect predictions using the formula  $(\text{True Positive} + \text{True Negative}) / (\text{True Positive} + \text{False Positive} + \text{True Negative} + \text{False Negative})$ . Lastly, specificity defines the ratio of true negative predictions against total negative predictions using the formula  $(\text{True Negative}) / (\text{True Negative} + \text{False Negative})$ . Where accurate predictions of a point's presence under 300 cm are considered true, and inaccurate predictions are considered false. Positive points are points predicted to have cryotic ground above 300 cm, and negative points are points that are not predicted to have cryotic ground above 300 cm.

### ***3.6 Determining local site influences on cryotic ground distribution***

Fifteen additional variables were collected at CAS, as described in 3.3 *Other field measurements*. These variables were compared with inferred cryotic ground presence at each CAS site as determined from the ALT extrapolation approach. To evaluate the importance of these local site characteristics for cryotic ground presence/absence, we applied the random forest machine learning technique. The 84 CAS points were split into training (70%, n= 60) and testing (30%, n= 24) samples for modelling. The default value of  $\sqrt{p}$  was used as the mtry (the number of random variables sampled at each split) for the random forest model. Where p = the number of variables the model was comparing. The default ntree (number of trees the model used) value of 500 was also used, as the dataset was relatively small with 84 points.

The model was iteratively run removing variables that decreased its accuracy. The variables that were reducing accuracy of the model can be determined through the output value of the random forest, "*mean decrease in accuracy*". The *mean*

*decrease in accuracy* is the measure on how much the accuracy decreases if a variable is excluded. A higher *mean decrease in accuracy* indicates a more correlated variable; the inverse of this is true as well. The lower the *mean decrease in accuracy*, the less correlated a variable is. If the *mean decrease in accuracy* is negative, it is actively reducing accuracy of a model and should be removed.

Two random forest models were used. One for the different types of vegetation, which can be seen in Figure 4.8 (herbaceous, moss, prostrate shrub, low shrub, high shrub, coniferous tree, lichen), and another for all other variables seen in Figure 4.4 (soil moisture, final depth reached with CAT probe, slope, percent cover of vegetation, max vegetation height, surficial materials, whether the site is disturbed, canopy cover, method of hole creation, whether or not the site had fill, drainage class, soil texture, organic layer thickness, and estimated snow cover.)

## Chapter 4: Results

### 4.1 Measured ground temperatures and evaluation of extrapolation methods

In total, data was collected from 84 CAS locations (Figure 4.1, Appendix A6). Seven points identified (CAS 1, 3, 4, 5, 11, 29, 38, and 41) had temperature measurements below 0°C, or frozen materials were directly detected with the frost probe (Figure 4.1, Appendix A6). The mean depth reached between all CAS was 123 cm and the mean temperature at its deepest point was 4.5°C. All CAS temperatures, depths, and variable data is located in Appendix A6 & A7.

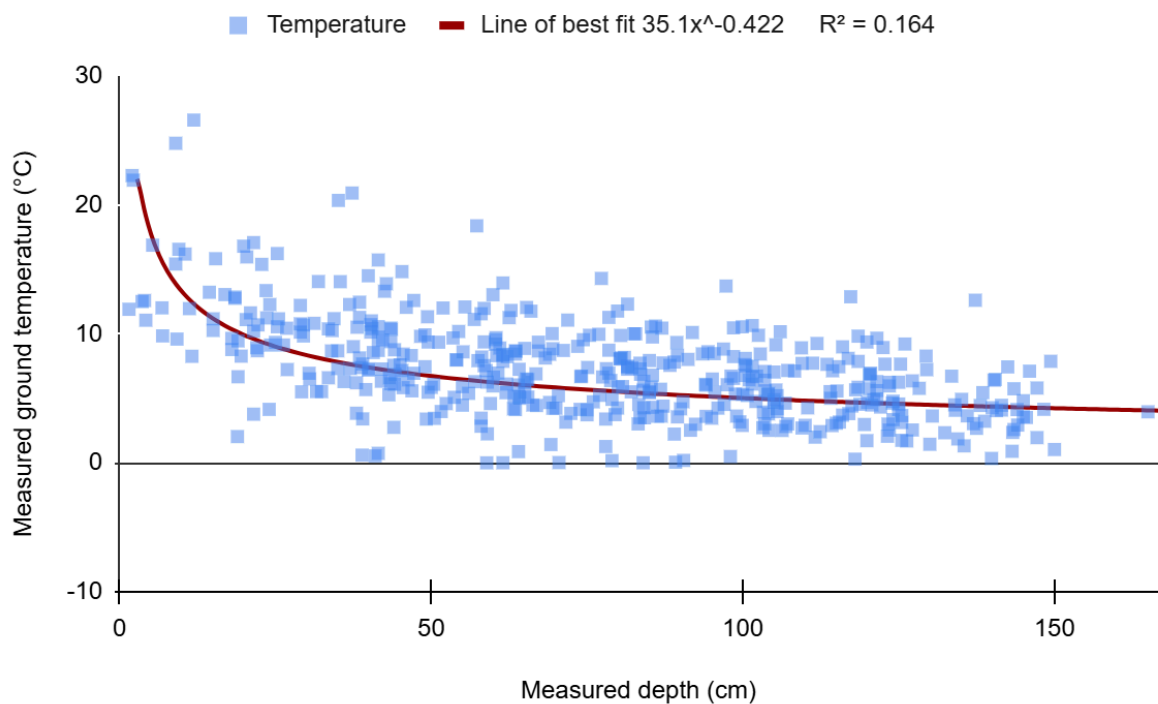


**Figure 4.1:** Results of all CAT probe readings in a graph with a power series trendline. Visualizes all ground temperature measurements. 8% of CAS points were at or below 0°C. The power series trendline had a lower  $R^2$  value, indicating that temperature and depth follow a nonlinear pattern. See Appendix A6 for all points.

From the simulated extrapolations we found that linear methods had accuracies ranging between 69 - 82% and an error ranging from  $\pm 38$  - 59 cm (Table 4.1). Polynomials had an accuracy between 74 - 83% and an error ranging from  $\pm 46$  - 86 cm (Table 4.1). LOESS had an accuracy of 86% and an error of  $\pm 27$  cm (Table 4.1). Finally, ALT had an accuracy of 99% and an error of  $\pm 48$  cm (Table 4.1). Therefore, the ALT method was determined to be the most accurate at determining the presence of cryotic ground despite its larger deviation for active layer thickness estimation (Table 4.1). The shallowest false positive for ALT was 291.967 cm, and so 300 cm was used as a cutoff for determining cryotic ground presence with this method. Due to its higher prediction accuracy, ALT was selected to be the main extrapolation method for the CAS data. However, LOESS had the lowest mean absolute error for active layer thickness prediction ( $\pm 27$  cm) when permafrost was present, and so the LOESS method was used for estimating active layer thickness when the ALT method determined cryotic ground was present.

Appendix A1 depicts the ALT extrapolation results. Every 'yes' is a prediction of permafrost presence under 300 cm using ALT. Above a third (38% 33/84) of points are predicted to have cryotic ground. Seven points identified in red had temperature measurements below 0°C, or frozen material was detected with the frost probe (Figure 4.1). Therefore, their result is not a prediction but is an example of confirmed cryotic ground presence.

Comparison of extrapolation methods In percent					
(A)	Linear (all points)	Linear (deepest 3 points)	Linear (deepest 2 points)	Linear (shallowest & deepest point)	ALT approach (modified from Uxa et al. 2026)
Mean absolute error of predicted active layer depth for true positives	±38 cm	±51 cm	±59 cm	±56 cm	±48 cm
Precision	0.68	0.74	0.75	0.68	<b>0.99</b>
Accuracy	0.82	0.86	0.87	0.69	<b>0.99</b>
Specificity	0.69	0.77	0.77	0.69	<b>0.99</b>
(B)	LOESS	2nd polynomial (all points)	2nd polynomial (deepest 3 points)	Mean of all methods	
Mean absolute error of predicted active layer depth for true positives	<b>±27 cm</b>	±46 cm	±86 cm	±52 cm	
Precision	0.74	0.61	0.74	0.74	
Accuracy	0.86	0.74	0.83	0.86	
Specificity	0.77	0.57	0.78	0.77	

**Table 4.1:** Results of extrapolation method comparison using simulated temperatures from Colyn et al. (2025). Red highlights the highest value for each category. Table separated into sections (A) and (B) for readability. \*The mean absolute error excludes all false positive results.

## 4.2 Cryotic assessment site results for Nain

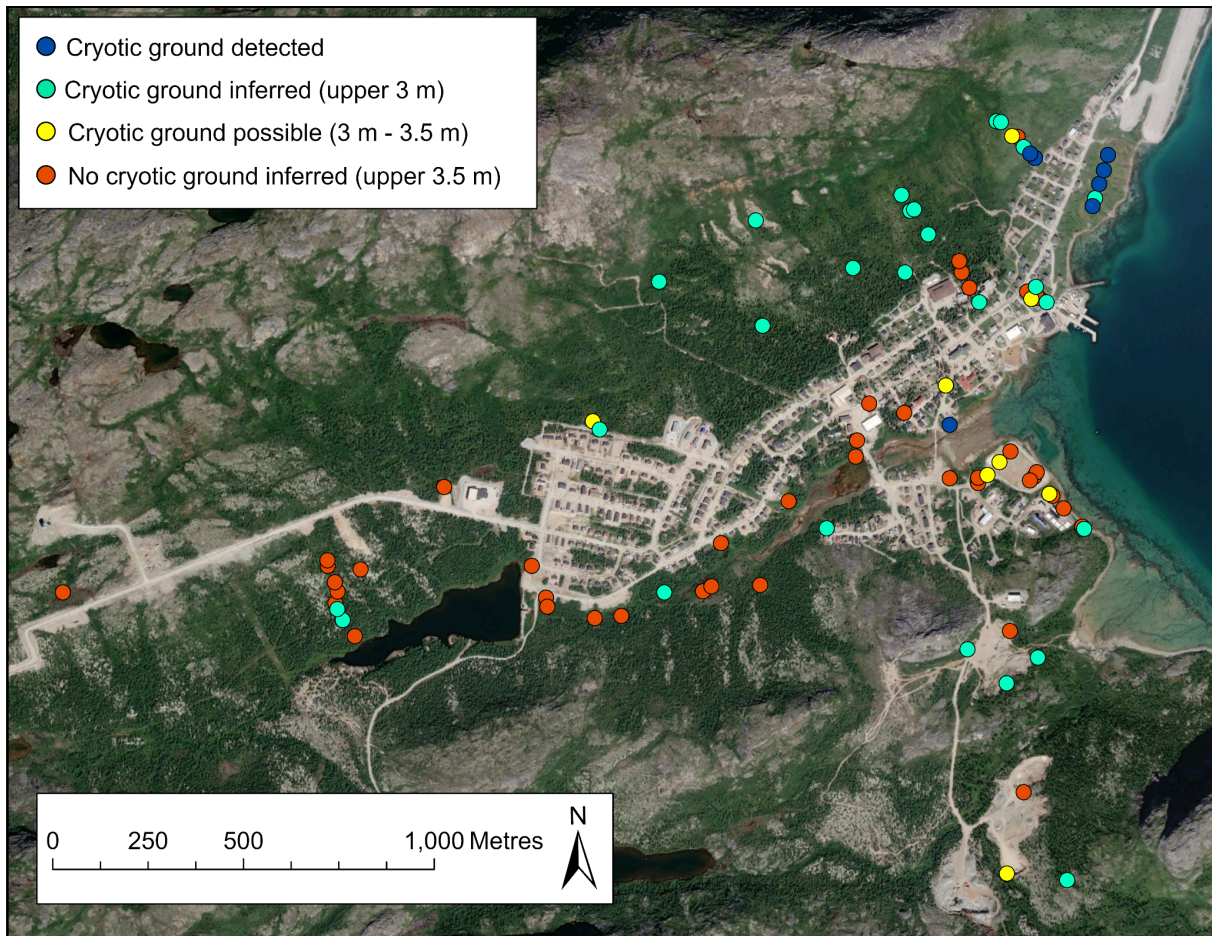


**Figure 4.2.** Map of CAS points and their predicted permafrost presence using ALT (see table 4.2).

The seven dark blue points labeled *Cryotic ground detected* are points that were measured cryotic with the CAT probe. The 26 cyan points labelled *Cryotic ground inferred (upper 3 m)* are points that ALT predicted would be cryotic under 3 m. The 8 yellow points labelled *Cryotic ground possible (3 m - 3.5 m)* are points that ALT predicted would be cryotic when the cutoff was increased from 3 m to 3.5 m. The 43 points labelled *No cryotic ground inferred (upper 3.5 m)* are points that ALT did not predict cryotic ground presence, even after the increased 3.5 m cutoff.

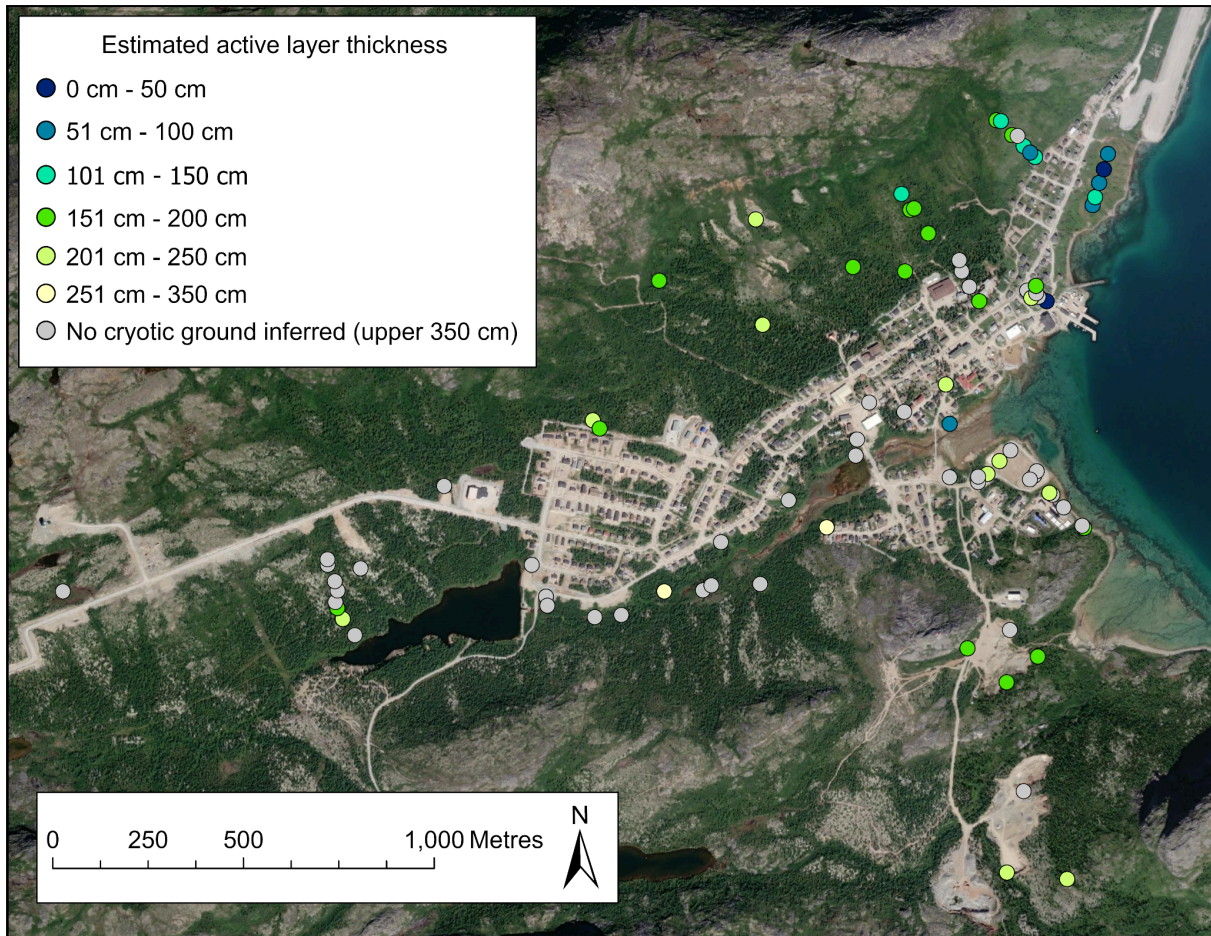


**Figure 4.3.** Map of CAS points and the predicted depth of the active layer using LOESS.

Active layer depth was predicted using LOESS. Areas predicted with permafrost presence from 0 - 350 cm in ALT had LOESS performed on the same points to predict depth. Out of all the points that predict permafrost presence in ALT, LOESS's depth prediction did not exceed 300 cm. LOESS predicted that CAS 84 had cryotic ground at 14 cm, which is physically impossible as ground temperature measurements reached 145 cm at 3.5°C. Therefore, at CAS 84, ALT's predicted depth of 299 cm was used instead.

## 4.2 Assessing variable correlation

### 4.2a Random forest for observed variables

Through the running of a random forest model three consecutive times, it was found that organic layer thickness, canopy cover, soil texture, and snow cover all have a negative *mean decrease in accuracy* (Figure 4.4). Figure 4.4 depicts the results of the first run of the random forest model. Variables were removed until no negative mean decreases in accuracy were present. The 4th iteration of the dataset will be used for further analysis and is what is present in all other random forest results of the non-vegetation variables.

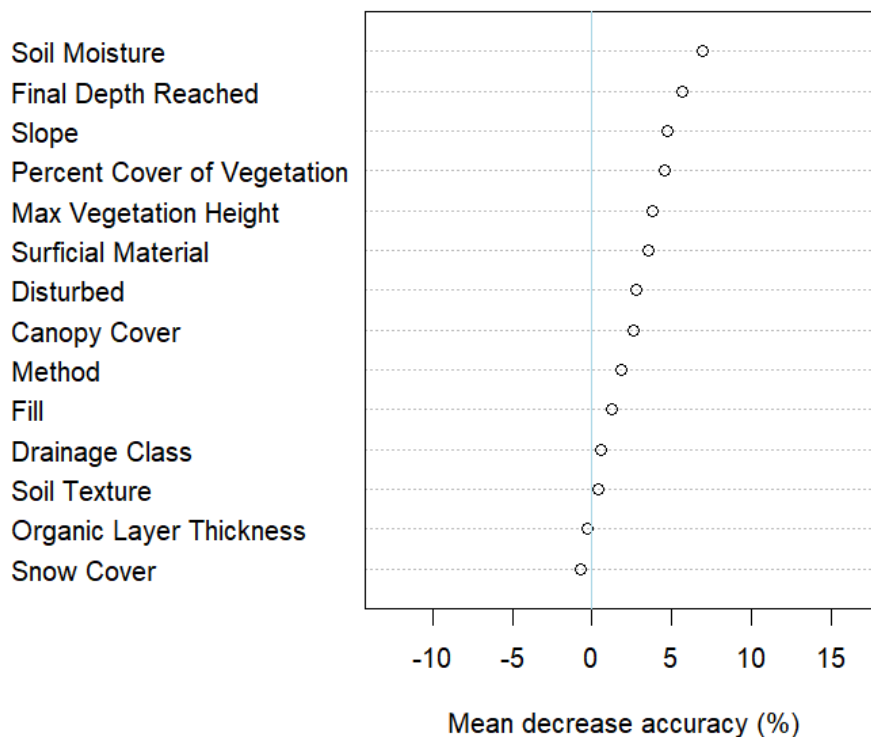


**Figure 4.4:** Graph of mean decrease accuracy of the first run of the forest model on observed variables.

The accuracy of estimates of both cryotic ground presence and cryotic ground absence is unequal, with an accurate prediction of cryotic ground absence at 81% and an accurate prediction of cryotic ground presence at 71% (Table 4.2).

**Table 4.2:** Confusion matrix depicting the output of the random forest model.

	Model not predicted present	Model predicted present	% error
Cryotic ground is not present	29	7	19%
Cryotic ground is present	7	17	29%
Estimate of error rate			23%

In practice, the error rate of estimating cryotic ground presence in the first 300 cm using observed variables is 6% larger than the error rate predicted by the random forest model (Table 4.3).

$$7 \text{ incorrect} / 24 \text{ predictions} = 0.29$$

Error rate using the model: 29%

**Table 4.3:** Table of results using the prediction model developed from the random forest model. “Chance of cryotic ground not present” and “Chance of cryotic ground presence” are the decimal percent chance the model predicts that cryotic ground is not present at that CAS. The Prediction column describes whether the model predicted presence based on which of the previous decimal percent chances is greater. The last column, “Does the extrapolation agree?” compares the prediction with the extrapolation results in appendix A1.

CAS number	Chance of cryotic ground not present	Chance of cryotic ground present	Prediction	Does the extrapolation agree?
5	0.216	0.784	present	yes
8	0.978	0.022	not present	yes
14	0.390	0.610	present	yes

16	0.828	0.172	not present	no
17	0.792	0.208	not present	yes
22	0.526	0.474	not present	no
23	0.978	0.022	not present	yes
26	0.588	0.412	not present	yes
28	0.622	0.378	not present	yes
30	0.658	0.342	not present	no
37	0.590	0.410	not present	no
40	0.594	0.406	not present	yes
45	0.654	0.346	not present	yes
47	0.654	0.346	not present	no
49	0.962	0.038	not present	yes
50	0.744	0.256	not present	yes
52	0.800	0.200	not present	yes
53	0.744	0.256	not present	yes
58	0.976	0.024	not present	yes
60	0.300	0.700	present	yes
63	0.398	0.602	present	no
66	0.442	0.558	present	no
81	0.608	0.392	not present	yes
82	0.720	0.280	not present	yes

Total disagreements:	7
----------------------	---

Figure 4.5, displays that the most important variables are the percent cover of vegetation and soil moisture. Using Figure 4.6c, we can determine that for percent cover of vegetation, 0 - 60% cover indicates a higher likelihood of cryotic ground to be predicted absent. The second most important indicator is soil moisture. Cryotic ground absence predictions are most dependent on hydric conditions. In total, Figure 4.6a Mesic, Figure 4.6d vegetation height from 50-100 cm, and Figure 7.7b final

depth of 0-110 cm are the most associated with predicted permafrost presence as they have the lowest dependence when the dependent variable is *no presence*.

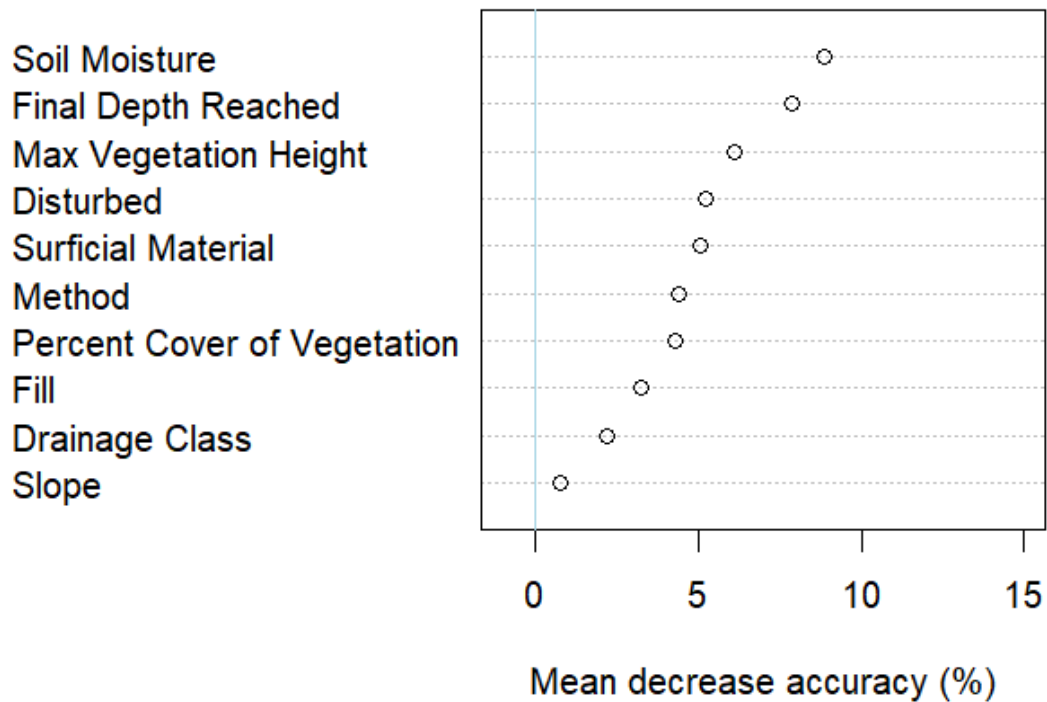


**Figure 4.5:** Graph of the mean decrease accuracy for variables (excluding plant types, snow cover, soil texture, canopy cover, and organic layer thickness)

The Y axis in Figure 4.6 (labelled dependence) represents values that only have meaning in relation to each other. Appendix A1 depicts this with the columns *Chance of cryotic ground not present* and *Chance of cryotic ground present*. Each variable contributes to the strength of the *not present* and *present* categories, providing a percent chance for each. Negative dependence, such as Mesic in Figure 4.6a, contributes to a *predicted presence* outcome. Notably the inverse versions of Figure 4.6a (which can be seen in Figure 4.7) represent the *present* dependent variable. Meaning that if hydric from Figure 4.6a is 0.7 when the dependent variable is *not present*, then it is -0.7 when the dependent variable is *present* (see Figure 4.7). As the y-axis in Figures 4.7 are relative to each other, negative and positive

dependence values do not imply a negative correlation to the model, it indicates a lower association. This also means that 0 does not indicate the middle ground between the association of variables.

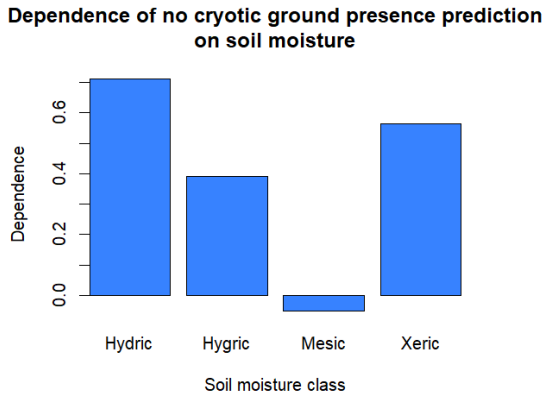


**Figure 4.6a:** Partial dependency plot soil moisture types.

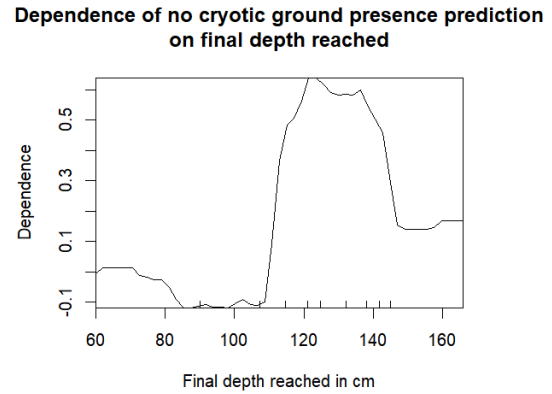


**Figure 4.6b** Partial dependency plot of final depth reached.

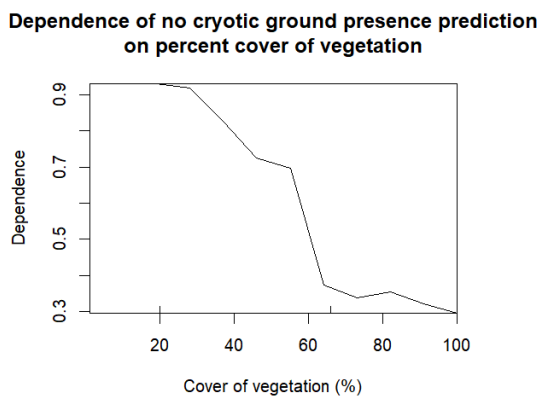


**Figure 4.6c:** Partial dependency plot of percent cover of vegetation.

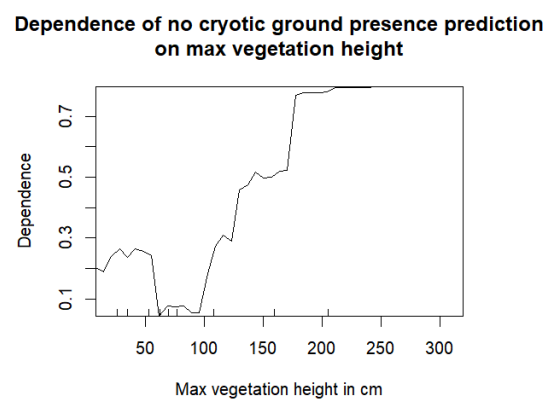


**Figure 4.6d:** Partial dependency plot on max vegetation height.

**Figure 4.6.** A series of plots depicting the partial dependence of the prediction of cryotic ground absence based on various variables. Where the dependent variable is no cryotic ground presence predicted. An explanation of each variable can be found in appendix A5 and remaining plots can be found in appendix A2.

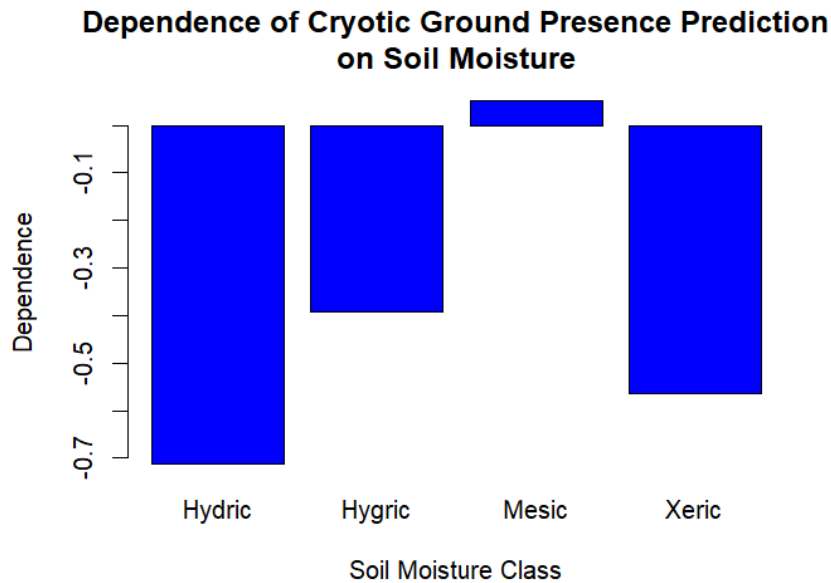


**Figure 4.7:** Figure 4.6a with the dependent variable changed to *present*.

#### 4.2b Random forest for vegetation

The random forest model for vegetation had an estimated error rate of 30% (Table 4.4). It was more accurate at predicting when cryotic ground was not present (78%) to when it was present (59%) (Table 4.4). Moss and low shrub were the most correlated with cryotic ground prediction, while deciduous trees and lichen were the least correlated (Figure 4.8). Appendix A3 depicts the partial dependence plots for all variables. From these plots it was concluded that moss, prostrate shrub, lichen, and low shrub to be associated with predicted permafrost presence and herbaceous and high shrub being associated with no permafrost predicted.

**Table 4.4:** Table depicting the output of the random forest model as a confusion matrix for vegetation types.

	Model not predicted present	Model predicted present	% error
Cryotic ground is not present	28	8	22%
Cryotic ground is present	9	14	41%
Estimate of error rate			30%

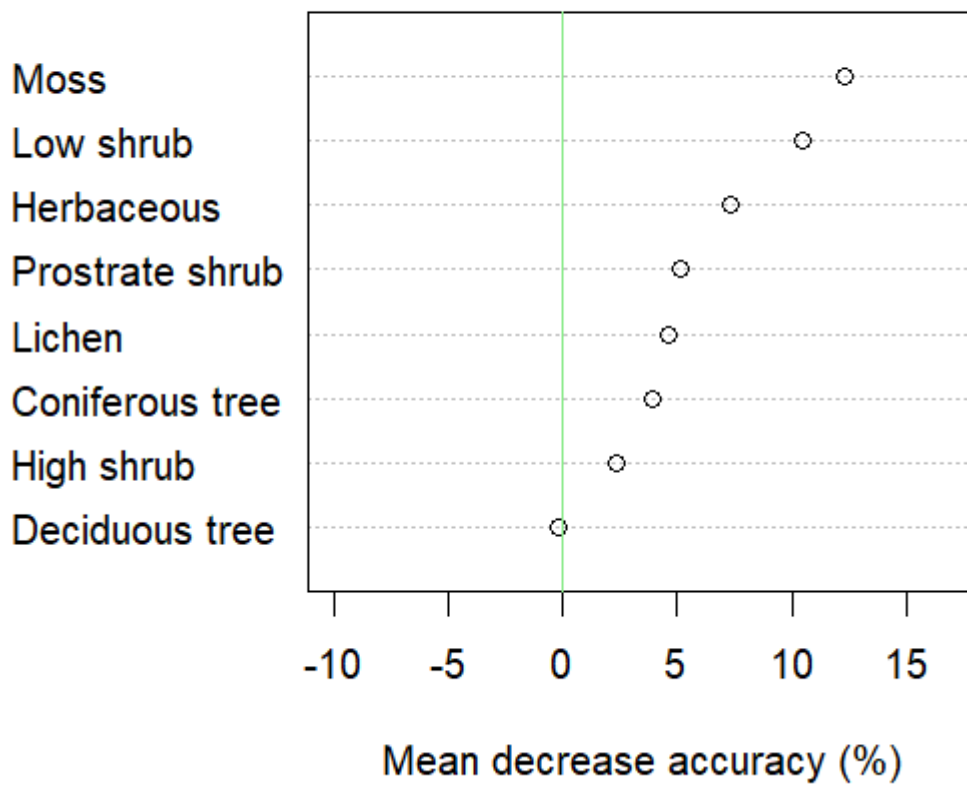


**Figure 4.8:** Mean decrease accuracy for vegetation types.

## Discussion

### ***5.1 Ground temperature measurements and regression results***

The CAS measurements resulted in 84 ground temperature gradients. All points were extrapolated to infer the depth of cryotic ground. Eight types of regressions were compared using modeled ground temperatures to evaluate which was the best fit for this project. We found that the ALT approach from Uxa et al. (2026) had the highest accuracy at extrapolating and predicting the presence of cryotic ground (Table 4.1). However, LOESS had the lowest mean absolute error (Table 4.1) for the subset of sites at which cryotic ground was present. Therefore, the ALT approach was used to determine the presence/absence of cryotic ground, and the LOESS approach was used to determine the depth to cryotic ground where it was inferred to be present. According to the predicted cryotic ground map (Figure 4.2), cryotic ground seems to be found or predicted to be present in undeveloped areas. This can be explained by the presence of structures and the clearing of vegetation in developed areas, which could have degraded previously present permafrost (Way et al. 2021). CAS 41, a site where we identified cryotic ground, was found to be near an old borehole with no cryotic ground (see Figure 3 in Way et al. 2021). The differences in temperatures between the two sites demonstrates significant spatial variability of cryotic ground presence in Nain.

These findings could have greater implications for cryotic ground detection using ground temperature measurements. Previous studies utilising ground temperature measurements to predict cryotic ground presence have used linear extrapolation for ground temperature measurements (Bonnaventure and Lewkowicz 2008, Daly et al. 2022, Nicholson 2025). Linear regressions had 69 - 87% accuracy

(Linear six points, Linear deepest three points, Linear deepest two points, Linear highest and deepest) when compared to our ensemble of modeled ground temperature data. By comparison, a modified version of the active layer thickness estimation approach from Uxa et al. (2026) had a 99% accuracy under 300 cm suggesting that widely used linear extrapolations are not the most accurate at predicting ground temperatures with depth. However, the depths of temperature measurements, the intervals of temperature measurements, and depth to extrapolation are different between this project and all other projects, which could change the accuracy (Riseborough 2008). Moreover, the modeling was performed based on temperature data for Labrador, and accuracy may change based on location. Therefore, future research may benefit from modeling the accuracy of regressions to find the most suitable method for unique environments.

## ***5.2 Influence of local site characteristics on CAS results***

Two variations of the random forest model were performed: one analysing the association between cryotic ground prediction and vegetation types found at CAS (Figure 4.8) and one analysing the relation between cryotic ground prediction and all other CAS variables collected in the field (Figure 4.6).

In terms of observed variables, it was found that soil moisture, the final depth reached by the CAT probe, and maximum vegetation height had the highest mean decrease in accuracy (Figure 4.5). This means that when these variables are removed from the model, the accuracy of the model predictions decreases by 6-10%. This makes these variables the most correlated with predicted cryotic ground

presence. Figure 4.6a depicts the correlation of soil moisture and predicted cryotic ground. It is observed that moist conditions (hydic and hygric), along with very dry conditions (xeric), have an association with no cryotic ground predicted. Slightly dry conditions (mesic) have a negative dependence, indicating it is associated with cryotic ground predictions. Most predicted depths of cryotic ground were extrapolated deeper than where soil moisture was evaluated. Permafrost impedes drainage of water resulting in an increase of moisture at the base of the active layer (Xiao et al. 2025). It can be inferred that the reason why mesic conditions are more correlated to permafrost presence is because higher moisture at these sites would be more likely at the base of the active layer. In the field, soil moisture conditions were only considered at the surface. Therefore, deeper depths of permafrost would not be the dominant mechanism for determining soil moisture. Instead, vegetation and terrain are likely larger indicators (Xiao et al. 2025). Therefore, mesic conditions may be a common trait of areas where cryotic ground was inferred and a result of an overall trend in terrain and vegetation.

Figure 4.6b depicts the dependence of the final depth of the CAT probe and permafrost not being predicted presence. Final depths of up to 110 cm are the most associated with predicting permafrost. This can have multiple reasons. All CAS where frozen ground was found with the frost probe, final depths were below 100 cm. This means that all CAS whose final depth is below 100 cm (except CAS 18) were measured to be cryotic. This is because the minimum depth recorded if cryotic ground was not found is 100 cm. As a result, after 110 cm, the dependence for no cryotic ground increases. Another reason measurement depths of 0 - 110 cm are less dependent is due to how temperature gradients develop. Figure 4.1 shows that temperature changes are not linear as depth increases. Therefore, larger intervals of

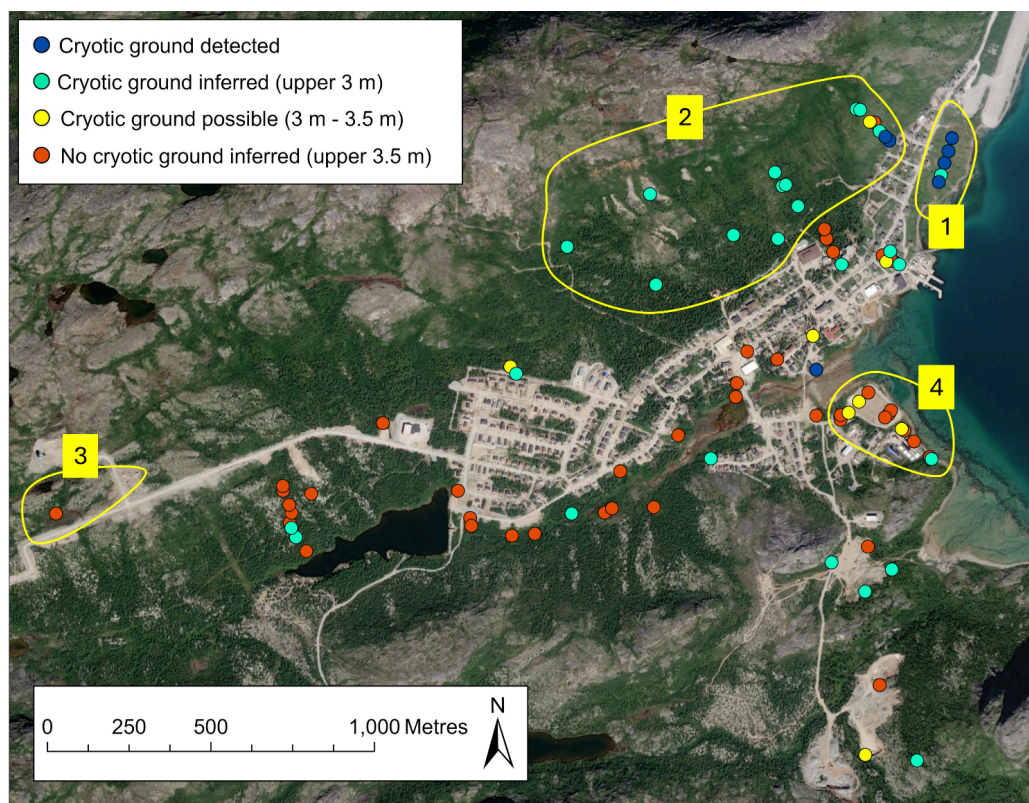
temperature readings are seen at shallower depths. Larger intervals can create steeper slopes for extrapolations. Therefore, if a deeper depth is not reached where the temperature curve begins to level, a higher likelihood of permafrost may be predicted. This means that to make more informed ground temperature decisions, it is important to reach the deepest depth possible.

Figure 4.6d depicts the dependence of max vegetation height on a non-cryotic ground prediction. We can observe that the lower the maximum vegetation height, the more likely cryotic ground is to be predicted. The vegetation results are in agreement with these findings, as the vegetation types associated with cryotic ground prediction characteristically have a low maximum height. These vegetation types include moss, prostrate shrub, lichen, and low shrub (appendix A3). This corroborates the idea that an increase in vegetation height can increase the insulating effect of snow in the winter, thereby increasing ground temperatures and decreasing permafrost presence (Heijmans et al. 2022). This implies that in Nain, the taller vegetation types contribute to snow trapping in the winter, insulating the ground and reducing permafrost presence.

### 5.3 Permafrost in the community of Nain, Nunatsiavut

In the context of literature this project is the first to examine permafrost presence outside the marine limit in Nain (Way et al. 2021). These investigations are important as the results of the CAS and the rest of the SISAdapt project can support informed infrastructure decisions. Figure 5.1 highlights these regions of interest.

Region 1, the foreshore, is a prospective development area due to its ideal location by the water. However, this area seems to be underlain by a long body of permafrost. This agrees with the ERT survey results in Way et al. (2021).



**Figure 5.1:** Map of cryotic ground presence divided into sections. 1) Foreshore 2) Hillslope 3) Potential development areas 4) The park.

Region 2, the hill north of the town, is of particular concern. The inferred cryotic ground temperatures here could indicate permafrost bodies on the hill. If it is ice-rich, thaw could be hazardous for the community. These predictions are not

definitive, and so these locations should be assessed for hazards even further to confirm whether this region is a cause for concern.

Region 3 is an area where new housing is potentially being built. Further west down the road, we attempted at many locations to take ground temperature measurements, but we had difficulty reaching our target depth due to the assumed bedrock. CAS (68) was the only site in this region where we were able to reach an appropriate depth. This could indicate that there is less ice-rich permafrost in this region. However, individual spots that may be used for construction merit further analysis as bodies can be discontinuous (as seen by the borehole and CAS 41 mentioned in section 5.1).

Visually, region 4, the park, appears to have undergone subsidence (Figure 5.2). The previously assumed flat baseball field has noticeable bumps, and certain features nearby, such as benches, fences and the gazebo, are tilted. It is assumed that some of this subsidence is due to thaw, as there are CAS that predict small sections of cryotic ground in this area. We predict that the spots that are labelled cryotic could be of two things. They are remnants of a previous larger body in this location, whose thaw has caused subsidence in the field or seasonal frost left over from the winter.



**Figure 5.2:** Oblique photo of region 4 collected with an uncrewed aerial vehicle. Differential subsidence is evident along the fence line of the park near the play structures.

#### ***5.4 Limitations and improvements***

A major limitation of the simulation data was that cryotic ground was often simulated to be present below 200 cm or above 400 cm. Therefore, our extrapolation approaches may be biased towards predicting cryotic ground that ranges outside 200 - 400 cm rather than within that range.

Seasonal frost may be another issue encountered. Due to Labrador's cold summers seasonal frost has the potential to persist long into the summer (Way et al. 2018, 2021). The ground temperature measurements taken at CAS cannot differentiate seasonal frost and permafrost. To avoid seasonal frost ground temperature measurements were taken later in the summer from late July to mid August, and co-located ERT data collection at some sites did allow us to interpret deeper in the ground at these locations. The dates each CAS was taken can be viewed in Appendix A6.

Another limitation was the comparison of frost probing and drilling holes to place the CAT probe into. Daly et al. (2022) hypothesized that the heat from the drill could potentially create a thermal disturbance at the drilling site so they decided to cap drill holes and wait 24 hours before temperature measurement. To test for this issue, two holes (one drilled, the other frost probed) were drilled ~50 cm adjacent for the purpose of comparing temperatures measured with both approaches. Temperatures measured with the CAT probes at these two parallel measurement sites were compared after fifteen minutes and no evidence of residual heat from drilling was found. However, typically the drill will be used in areas that the frost probe could not penetrate. Meaning that coarser, harder to penetrate substances, take much longer to drill and create potentially more heat than our tested areas. A temperature test within difficult to drill sediments would be more useful. It is important to mention that we did have two CAS (CAS 11 & 7) where drilling occurred, and the sites were capped and measured ten and one day later respectively; they were not the most difficult spots to penetrate, and the new temperature measurements did not change the conclusions of the extrapolation.

The sample size for variables was also a limitation. Because the results of the variables at CAS were not predetermined, an equal sample size of each type of variable was not present. This led to variables having disproportionate amounts of different classes. As an example, for soil moisture, there are 12 hydric points but 31 mesic points. This disproportionate sample can skew results based on the randomness of the random forest, but also change sensitivities for each category.

## 5.5 Future work

This project has identified a few areas of interest for future work. Further investigation on the hillslope 2) in Figure 5.1 should be a priority to ensure that there are no potential hazards in the area. This project also found that linear extrapolation was not the most effective at predicting cryotic ground. This was done using modeling based on climate data from Labrador. Investigations on whether these findings are equally applicable to other regions may also be useful for future ground temperature projects.

## Chapter 6: Conclusion

In the face of climate change, permafrost environments such as in coastal Labrador are changing. The community of Nain is in need of rapid infrastructure development to support its growing population. Geocryological hazard mapping is required to support this urgent infrastructure development. A part of this mapping was done using 84 CAS to assess permafrost absence and presence, as well as to assess the drivers of permafrost distribution in the community. We found that 33/84 CAS predicted or detected cryotic ground presence. Results indicate that these locations were primarily found in undeveloped locations outside of the existing community. Notably, cryotic ground was predicted to be present on the hillslope north of the airport, suggesting a potential hazard that will require further investigation. The vegetated plot south of the airport also measured substantial cryotic ground presence, indicating that any further development in the area may require mitigation strategies to address thaw. Through CAS, cryotic ground presence was inferred across Nain and will aid in mapping of permafrost presence.

## References

- Bell, T., P t, M., Sheldon, T., 2011. Landscape hazard assessment in Nain, Phase 1: Inventory of surficial sediment types and infrastructure damage (Technical report). Nunatsiavut GoverBoike, J., Chadburn, S., Martin, J., Zwieback, S., Althuizen, I.H.J., Anselm, N., Cai, L., Coulombe, S., Lee, H., Liljedahl, A.K., Schneebeli, M., Sjöberg, Y., Smith, N., Smith, S.L., Streletskiy, D.A., Stuenzi, S.M., Westermann, S., and Wilcox, E.J. 2022. Standardized monitoring of permafrost thaw: a user-friendly, multiparameter protocol. *Arctic Science*, 8(1): 153–182. NRC Research Press. doi:10.1139/as-2021-0007.
- Bonnaventure, P.P., and Lewkowicz, A.G. 2008. Mountain permafrost probability mapping using the BTS method in two climatically dissimilar locations, northwest Canada. *Canadian Journal of Earth Sciences*, 45(4): 443–455. NRC Research Press. doi:10.1139/E08-013.
- Colyn, V. 2024. INVESTIGATING THE VARIABILITY OF GROUND TEMPERATURES ACROSS COASTAL-CONTINENTAL AND LATITUDINAL GRADIENTS IN LABRADOR, NORTHEASTERN CANADA. Queen's University, Kingston, Ontario.
- Colyn, V., Way, R., Wang, Y., Beer, J., Trant, A., Hermanutz, L., Forget, A., Tutton, R., Barone, K., Power, M., Fedder, L., Rendell, E., Gaul, N., and Le, N. 2025. Investigating spatial variability of ground temperatures across coastal and continental highlands in Labrador, northeastern Canada. *Arctic Science*, 11: 1–26. NRC Research Press. doi:10.1139/as-2024-0079.
- Daly, S.V., Bonnaventure, P.P., and Kochtitzky, W. 2022. Influence of ecosystem and disturbance on near-surface permafrost distribution, Whatì, Northwest Territories, Canada. *Permafrost and Periglacial Processes*, 33(4): 339–352. doi:10.1002/ppp.2160.
- Environment Canada. 2025. Canadian Climate Normals 1981-2010 Station Data-Nain A.
- Fortier, R., and Bolduc, M. 2008. THAW SETTLEMENT OF DEGRADING PERMAFROST: A GEOHAZARD AFFECTING THE PERFORMANCE OF MAN-MADE INFRASTRUCTURES ATUMIUJJAQ IN NUNAVIK (QUÉBEC).
- GRID-Arendal. 2020. NORTHERN ISSUES, SCIENCE GAPS AND RECOMMENDATIONS. Available from <https://storymaps.arcgis.com/stories/74bf8d1540c542b7a444a5a2ba1559e2>. [accessed 22 October 2025].
- Heijmans, M.M.P.D., Magnússon, R.Í., Lara, M.J., Frost, G.V., Myers-Smith, I.H., van Huissteden, J., Jorgenson, M.T., Fedorov, A.N., Epstein, H.E., Lawrence, D.M., and Limpens, J. 2022. Tundra vegetation change and impacts on permafrost. *Nature Reviews Earth & Environment*, 3(1): 68–84. Nature Publishing Group. doi:10.1038/s43017-021-00233-0.

- Herring, T., Lewkowicz, A.G., Hauck, C., Hilbich, C., Mollaret, C., Oldenborger, G.A., Uhlemann, S., Farzamian, M., Calmels, F., and Scandroglio, R. 2023. Best practices for using electrical resistivity tomography to investigate permafrost. *Permafrost and Periglacial Processes*, 34(4): 494–512. doi:10.1002/ppp.2207.
- Holloway, J.E., and Lewkowicz, A.G. 2020. Half a century of discontinuous permafrost persistence and degradation in western Canada. *Permafrost and Periglacial Processes*, 31(1): 85–96. doi:10.1002/ppp.2017.
- Hugh M. French and Olav Slaymaker. 2012. *Changing Cold Environments : A Canadian Perspective*. Wiley-Blackwell, Chichester.
- Lafrenière, M.J., and Lamoureux, S.F. 2019. Effects of changing permafrost conditions on hydrological processes and fluvial fluxes. *Earth-Science Reviews*, 191: 212–223. doi:10.1016/j.earscirev.2019.02.018.
- Langer, M., von Deimling, T.S., Westermann, S., Rolph, R., Rutte, R., Antonova, S., Rachold, V., Schultz, M., Oehme, A., and Grosse, G. 2023. Thawing permafrost poses environmental threat to thousands of sites with legacy industrial contamination. *Nature Communications*, 14: 1721. doi:10.1038/s41467-023-37276-4.
- MacKenzie, W., Kennedy, C., and Flynn, N. 2022. *Ecosystems of the Yukon Arctic Region A Guide to Identification*. Government of Yukon, Whitehorse, Yukon.
- Nicholson, R. 2025. EXAMINING PERMAFROST DETECTION AND VALIDATION TECHNIQUES IN THERMALLY COMPLEX MOUNTAINOUS TERRAIN: A CASE STUDY IN THE OGILVIE MOUNTAINS, YUKON, CANADA.
- Patton, A.I., Rathburn, S.L., Capps, D.M., McGrath, D., and Brown, R.A. 2021. Ongoing Landslide Deformation in Thawing Permafrost. *Geophysical Research Letters*, 48(16): e2021GL092959. doi:10.1029/2021GL092959.
- Power, M., Way, R.G., and Yifeng, W. 2025. Permafrost and geocryological hazard research trends in Nunatsiavut, northeastern Canada. p. 9.
- Riseborough, D.W. 2008. Estimating Active Layer and Talik Thickness from Temperature Data-Implication from Modeling Results. Fairbanks, Alaska, United States of America. pp. 1487–2492.
- Silavut Asianguvalliajuk Nunatsiavut Climate Change Workshop. 2024. *Nunatsiavut Government, Nain, Nunatsiavut*.
- Smith, S.L., Wolfe, S.A., Riseborough, D.W., and Nixon, F.M. 2009. Active-layer characteristics and summer climatic indices, Mackenzie Valley, Northwest Territories, Canada. *Permafrost and Periglacial Processes*, 20(2): 201–220. doi:10.1002/ppp.651.
- Streletskiy, D.A., Shiklomanov, N.I., Little, J.D., Nelson, F.E., Brown, J., Nyland, K.E., and Klene, A.E. 2017. Thaw Subsidence in Undisturbed Tundra Landscapes,

- Barrow, Alaska, 1962–2015. *Permafrost and Periglacial Processes*, 28(3): 566–572. doi:10.1002/ppp.1918.
- Tutton, R., Way, R., Beddoe, R., Zhang, Y., and Trant, A. 2021. Soil temperature sensitivity to variable snow and vegetation conditions in low-relief coastal mountains, Nunatsiavut and NunatuKavut, Labrador. In 2021 Regional Conference on Permafrost & 19th International Conference on Cold Regions Engineering. American Society of Civil Engineers. Boulder, Colorado, USA. pp. 71–81.
- Uxa, T., Hrbáček, F., and Kňázková, M. 2026. Simple analytical–statistical models (ASMs) for mean annual permafrost table temperature and active-layer thickness estimates. *The Cryosphere*, 20(1): 97–112. Copernicus GmbH. doi:10.5194/tc-20-97-2026.
- Wang, Y., and Way, R.G. 2025. Future Trajectories of Peatland Permafrost Under Climate and Ecosystem Change in Northeastern Canada. *Journal of Geophysical Research: Earth Surface*, 130(2): e2024JF007930. doi:10.1029/2024JF007930.
- Way, R.G., Lewkowicz, A.G., Wang, Y., and McCarney, P. 2021. Permafrost Investigations below the Marine Limit at Nain, Nunatsiavut, Canada. *Regional Conference on Permafrost 2021 and the 19th International Conference on Cold Regions Engineering*,: 11.
- Way, R.G., Lewkowicz, A.G., and Zhang, Y. 2018. Characteristics and fate of isolated permafrost patches in coastal Labrador, Canada. *The Cryosphere*, 12(8): 2667–2688. Copernicus GmbH. doi:10.5194/tc-12-2667-2018.
- Xiao, Y., Hu, G., Zhao, L., Du, E., Li, R., Wu, T., Wu, X., Liu, G., Zou, D., Xing, Z., Zhou, N., and Wu, Y. 2025. Vegetation and permafrost interactions shape soil moisture stratification in marginal permafrost zones. *Geoderma*, 464: 117596. doi:10.1016/j.geoderma.2025.117596.
- Zhang, T. 2005. Influence of the seasonal snow cover on the ground thermal regime: An overview. *Reviews of Geophysics*, 43(4). doi:10.1029/2004RG000157.
- Zhang, Y., Chen, W., and Cihlar, J. 2003. A process-based model for quantifying the impact of climate change on permafrost thermal regimes. *Journal of Geophysical Research: Atmospheres*, 108(D22). doi:10.1029/2002JD003354.

## Appendices

### Appendix A1

CAS number	Depth 1	Depth 2	Temperature at depth 1	Temperature at depth 2	ALT prediction	Cryotic ground predicted?
1	79.00	59.00	0.161	2.241	86	yes
2	139.9	119.9	0.334	1.713	155	yes
3	84.00	64.0	-0.002	0.864	89	yes
4	58.9	38.9	-0.006	0.593	62	yes
5	61.5	41.50	-0.001	0.734	57	yes
6	150.0	130.0	1.027	1.432	260	yes
7	115.0	95.00	3.066	3.457	438	no
8	133.5	113.5	6.713	7.633	435	no
9	137.0	117.0	3.033	3.811	302	no
10	165.0	145.0	3.950	4.809	358	no
11	118.0	98.00	0.276	0.483	179	yes
12	89.00	69.00	2.221	4.673	133	yes
13	62.00	42.00	5.432	6.322	315	no
14	75.00	55.00	3.722	4.462	285	yes
15	78.00	58.00	3.388	3.457	2052	no
16	121.0	101.0	4.888	6.427	257	yes
17	116.0	87.00	8.986	10.44	488	no
18	89.00	69.00	7.812	8.414	617	no
19	121.5	101.50	6.293	6.668	802	no
20	114.4	94.40	7.132	8.605	317	no
21	116.90	96.90	8.094	8.813	576	no
22	99.00	79.00	3.619	4.919	219	yes
23	140.0	120.0	4.266	4.676	565	no
24	129.5	109.5	7.218	7.702	735	no
25	138.5	118.5	5.439	5.853	673	no
26	134.0	114.0	4.489	5.514	318	no
27	144.0	124.0	4.126	4.624	485	no

28	145.5	125.5	3.513	3.660	1111	no
29	90.50	70.50	0.182	0.014	62	yes
30	135.5	125.5	1.31	1.737	201	yes
31	125.5	105.5	3.124	5.202	194	yes
32	146.0	126.0	7.100	9.204	290	yes
33	109.5	89.5	2.694	3.559	243	yes
34	143.3	123.3	2.354	2.999	298	yes
35	137.3	117.3	12.6	12.87	2013	no
36	137.5	117.5	2.671	4.400	208	yes
37	138.8	118.8	3.22	4.535	245	yes
38	143.2	123.2	0.89	2.052	181	yes
39	140.3	120.3	6.404	6.802	793	no
40	149.4	129.4	7.866	8.270	938	no
41	89.20	69.20	0.042	1.413	93	yes
42	134.1	114.1	4.072	4.998	319	no
43	120.4	100.4	6.917	8.090	365	no
44	111.9	91.9	9.246	10.10	554	no
45	142.5	122.5	7.432	8.932	350	no
46	141.5	121.5	4.455	5.601	306	no
47	148.3	128.3	4.144	5.772	259	yes
48	140.5	120.5	6.465	6.919	719	no
49	140.7	120.7	4.04	4.478	519	no
50	143.5	123.5	2.576	2.532	340	no
51	141.5	121.5	4.089	4.952	340	no
52	125.3	105.3	7.649	9.141	339	no
53	115.4	95.40	7.445	8.462	417	no
54	130.4	110.4	3.623	4.258	368	no
55	124.1	104.1	4.775	5.371	454	no
56	121.5	101.5	9.659	10.64	525	no
57	122.8	102.8	7.644	8.431	521	no

58	119.9	99.9	9.362	10.54	447	no
59	136.0	116.0	3.638	3.692	2840	no
60	138.1	118.1	4.441	5.657	293	yes
61	134.5	114.3	1.848	2.885	215	yes
62	122.1	102.1	4.319	4.752	530	no
63	147.2	127.2	5.796	6.347	577	no
64	111.2	91.2	7.721	8.013	1178	no
65	102.2	82.2	6.723	7.37	527	no
66	105.3	85.3	5.642	5.868	1113	no
67	135.1	115.1	4.914	5.565	446	no
68	123.5	103.5	5.957	6.4	671	no
69	111.6	91.6	1.984	2.522	268	yes
70	126.3	106.3	1.691	2.507	218	yes
71	106.9	86.9	2.815	3.614	257	yes
72	106.8	86.8	4.621	5.698	287	yes
73	103.6	83.6	5.577	6.857	287	yes
74	118.5	98.5	7.857	8.233	964	no
75	125.0	105	4.126	4.684	430	no
76	119.5	99.5	2.967	3.172	708	no
77	132.4	112.4	2.327	2.409	1277	no
78	144.1	124.1	2.923	3.342	432	no
79	143.5	123.5	5.737	6.236	613	no
80	104.2	84.2	2.512	3.487	216	yes
81	120.3	100.3	5.738	6.766	353	no
82	118.5	98.5	9.817	10.46	739	no
83	147.2	127.2	1.949	2.542	288	yes
84	145.0	125.0	3.571	4.556	299	yes

**Table A1:** CAT probe measurements of the two deepest points with ALT's depth of cryotic layer prediction. All points ALT predicts < 300 cm are predicted cryoitc. See appendix A6 for all points.

Appendix A2:

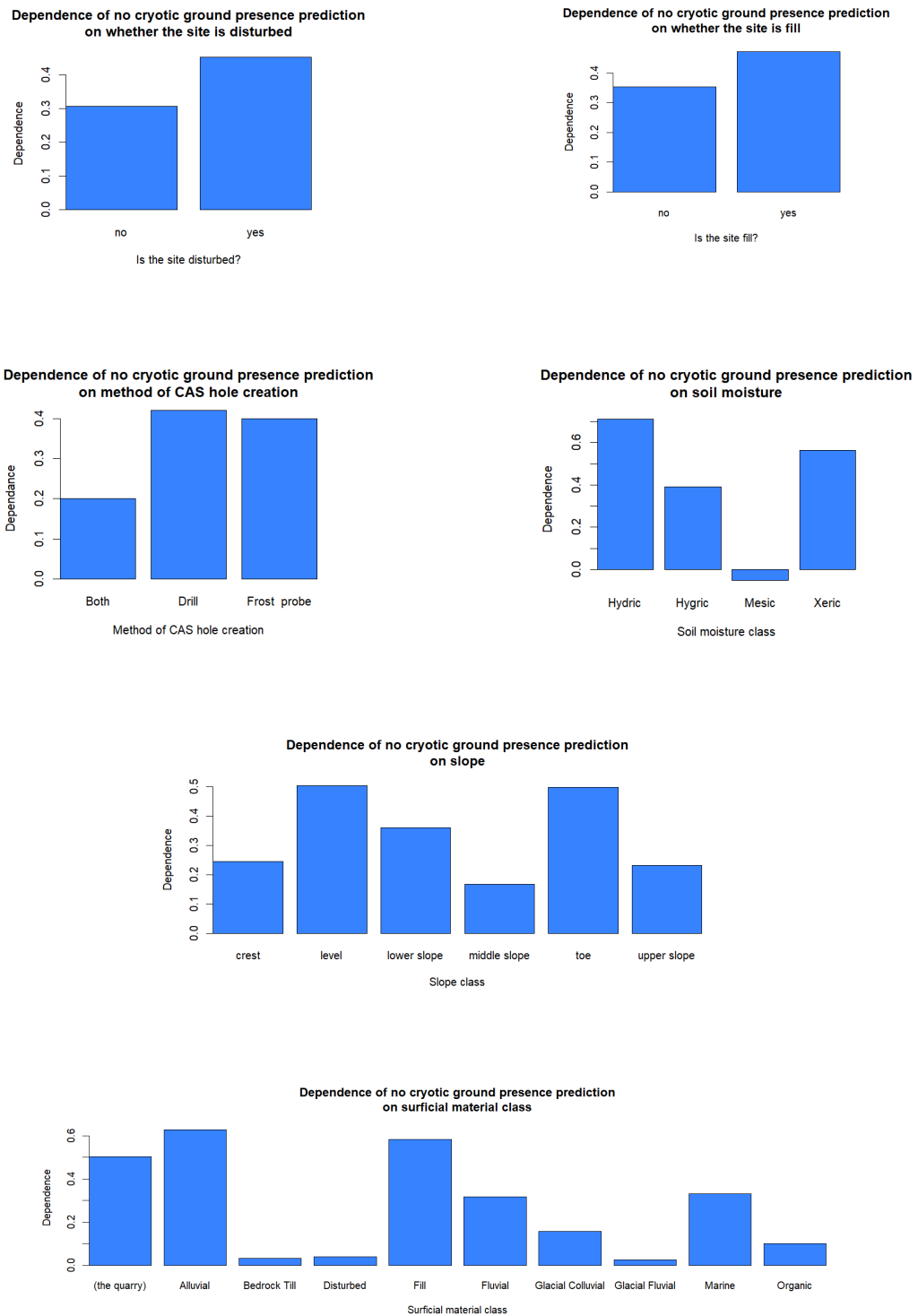


**Figure A1:** Remaining partial dependence of the prediction of cryotic ground absence based on various variables. Where the dependent variable is no cryotic ground presence predicted.

### Appendix A3

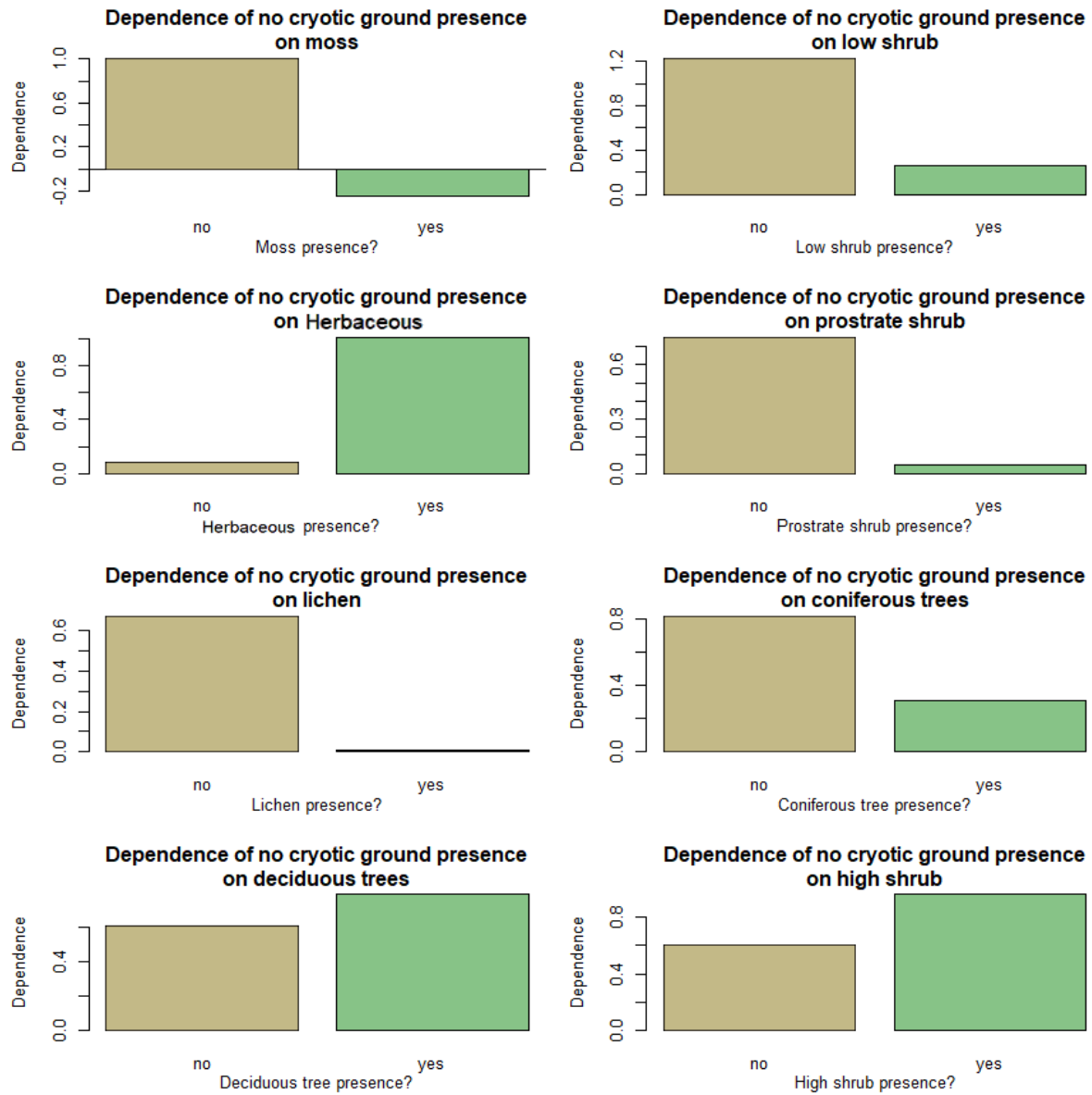


**Figure A3:** Series of partial dependence plots for vegetation types at CAS. Where the dependent variable is no cryotic ground presence predicted.

## Appendix A4 Cryotic Assessment Site Sheet 2025

### Collectors

Name(s): \_\_\_\_\_

### Site Info

<b>Site Name:</b>	Name: _____ Number: _____
<b>Method:</b>	Frost probe / Hand drill / Other _____
<b>Date:</b>	Month: _____ Day: _____
<b>Photos:</b>	Device Used: _____ Device Owner: _____
<b>GPS Coordinates:</b> <i>(to 6 decimal degrees)</i>	Site name: _____ Latitude: ____ . _____ °N Longitude: ____ . _____ °W
<b>Start &amp; end Time</b> <i>(in 24 hour format; hh:mm)</i>	Start Time: ____ : ____ End Time: ____ : ____
<b>Site Weather Conditions:</b> <i>(raining, snow, etc.)</i>	
<b>Weather History:</b> <i>(raining, snow, etc. the previous day)</i>	
<b>Elevation:</b> <i>(in metres above sea level)</i>	_____ . ____ m . a. s. l.
<b>Site Changes:</b> <i>(changes in site conditions between visits)</i>	

### General Collected Data

<b>Avg. Air Temperature:</b> <i>(one decimal, °C)</i>	<b>Organic layer thickness:</b>	<b>Max Vegetation height:</b>	<b>Percent cover of vegetation:</b>	<b>Disturbed?:</b>	<b>Fill?:</b>	<b>Canopy cover:</b>
____ . ____ °C	_____ cm	_____ cm	_____ %	Yes / no	Yes / no	_____ %
<b>Soil Moisture:</b> <i>(circle all that apply)</i>		Xeric / Mesic / Hygric / Hydric				
<b>Soil texture:</b> <i>(circle all that apply)</i>		Clay / Silt / Sand / Loam				

<b>Surficial Materials:</b> <i>(circle all that apply)</i>	Organic / Eolian / Lacustrine / Fluvial / Weathered Bedrock / Colluvial / Glacial / Marine
<b>Vegetation:</b> <i>(circle all that apply)</i> <i>(1m<sup>2</sup> box around point)</i>	Moss / Lichen / Low shrub / High shrub / Prostrate shrub Tree (deciduous) / Tree (coniferous) / Herbaceous Other: _____
<b>Snow cover:</b> <i>(circle all that apply)</i>	very exposed / exposed / neutral protected / very protected
<b>Drainage Class:</b>	poor / moderate / rapid
<b>Slope:</b> <i>(circle all that apply)</i>	crest / upper slope / middle slope / lower slope toe / depression / level

	Time: ____ : ____ Month: _____ Day: _____	
<b>Measurement time:</b> <i>(amount of time taken when measuring temperature)</i>	____ : ____	
<b>Temperature at depth:</b>	<b>Depth</b>	<b>Temperature</b>
	_____ cm	_____ °C
	_____ cm	_____ °C
	_____ cm	_____ °C
	_____ cm	_____ °C
	_____ cm	_____ °C
	_____ cm	_____ °C

**Figure A4:** Sheet used to document CAS information in the field.

## Appendix A5

Variable	Unit	Description
Organic Layer Thickness	cm	Measured Organic layer thickness with measuring tape.
Max vegetation height	cm	Maximum height of vegetation in a 50 cm radius from CAS hole.
Percent cover of vegetation	%	Surface cover of vegetation in a 50 cm radius from CAS hole.
Disturbed	Categorical	Whether or not the site appeared disturbed from anthropogenic activity.
Fill	Categorical	Whether or not the CAS was in fill.
Canopy cover	%	Amount of canopy cover above CAS in a 50 cm radius.
Soil moisture	categorical	Surface soil (under the organic layer) was evaluated for moisture. Determined using table A5-3 from (MacKenzie et al. 2022) and reduced the categories to Xeric, Mesic, Hygric, and Hydric.
Soil Texture	Categorical	Determined using the guide A5-2 Soil texture flow chart (MacKenzie et al. 2022).
Surficial material class	Categorical	Surficial class was based on the map from (Bell 2011).
Vegetation	Categorical	Based on observation in a 50 cm radius from CAS. Categories include moss, lichen, low shrub, high shrub, prostrate shrub, tree (deciduous), tree (coniferous), and herbaceous.
Snow Cover	Categorical	Based on how protected the CAS seemed to be based on hill position, vegetation, and wind exposure. Included categories of very exposed, exposed, neutral, protected,

		very protected.
Drainage class	Categorical	Determined using table A5-6 Drainage class codes and descriptions from (MacKenzie et al. 2022). Categories were reduced to poor, moderate, and rapid.
Slope	Categorical	Determined using Figure A5-1 Mesoslope position from (MacKenzie et al. 2022).

**Table A5:** Descriptions of how variables were collected in the field.

## Appendix A6

CAS number	Date	Longitude	Latitude	1 Depth	2 Depth	3 Depth	4 Depth	5 Depth	6 Depth	1 Temp	2 Temp	3 Temp	4 Temp	5 Temp	6 Temp
1	2025/07/25	-61.68659685	56.54622809	79	59	39	19	-1	-21	0.161	2.241	3.4	6.668	18.31	19.29
2	2025/07/25	-61.68648585	56.54641287	139.9	119.9	99.9	79.9	59.9	39.9	0.334	1.713	2.897	4.245	5.957	7.182
3	2025/07/25	-61.68629788	56.54674262	84	64	44	24	4	-16	-0.002	0.864	2.746	4.139	12.58	16.47
4	2025/07/25	-61.68609612	56.54706399	58.9	38.9	18.9	-1.1	-21.1	-41.1	-0.006	0.593	2.03	11.73	15.92	16.63
5	2025/07/25	-61.68590164	56.5474241	61.5	41.5	21.5	1.5	-18.5	-38.5	-0.001	0.734	3.766	11.9	16.41	16.8
6	2025/07/26	-61.68719713	56.53862276	150	130	110	90	70	50	1.027	1.432	2.903	4.182	4.234	5.844
7	2025/07/26	-61.68728184	56.53867874	115	95	75	55	35	15	3.066	3.457	4.107	5.905	8.681	11.16
8	2025/07/26	-61.6885212	56.53942117	133.5	113.5	93.5	73.5	53.5	33.5	6.713	7.633	8.44	9.025	9.678	10.38
9	2025/07/26	-61.68865654	56.5394642	137	117	97	77	57	37	3.033	3.811	4.523	5.23	6.285	7.311
10	2025/07/27	-61.688085	56.53912	165	145	125	105	85	65	3.95	4.809	6.244	7.034	7.926	8.867
11	2025/07/28	-61.68901042	56.54738706	118	98	78	58	38	18	0.276	0.483	1.259	2.833	3.84	8.779
12	2025/07/28	-61.68949818	56.54764903	89	69	49	29	9	-11	2.221	4.673	7.448	10.77	24.77	20.17
13	2025/07/28	-61.68998006	56.54791017	62	42	22	2	-18	-38	5.432	6.322	8.918	22.27	15.21	14.7
14	2025/07/28	-61.69063014	56.54826954	75	55	35	15	-5	-25	3.722	4.462	7.307	10.26	12.67	13.24
15	2025/07/28	-61.68974143	56.54788782	78	58	38	18	-2	-22	3.388	3.457	6.203	9.645	22.6	15.75

16	2025/0 7/29	-61.68863915	56.54398372	121	101	81	61	41	21	4.888	6.427	8.169	8.898	0.53	11.62
17	2025/0 7/29	-61.68898276	56.54408817	116	87	58	29	0	-29	8.986	10.44	11.55	12.2	12.78	13.54
18	2025/0 7/29	-61.68916048	56.54415017	89	69	49	29	9	-11	7.812	8.414	9.92	10.13	15.41	18.59
19	2025/0 7/29	-61.68945531	56.5442396	121.5	101.5	81.5	61.5	41.5	21.5	6.293	6.668	7.394	7.865	8.71	10.2
20	2025/0 8/06	-61.689294	56.54406497	114.4	94.4	74.4	54.4	34.4	14.4	7.132	8.605	9.539	10.18	11.17	13.22
21	2025/0 8/06	-61.68907457	56.54417619	116.9	96.9	76.9	56.9	36.9	16.9	8.094	8.813	9.96	11.109	12.27	13.04
22	2025/0 8/06	-61.68907569	56.54434504	99	79	59	39	19	-1	3.619	4.919	6.252	7.658	9.45	16.34
23	2025/0 8/04	-61.71022121	56.53724847	140	120	100	80	60	40	4.266	4.676	5.309	5.882	6.639	7.281
24	2025/0 8/04	-61.71016446	56.5370302	129.5	109.5	89.5	69.5	49.5	29.5	7.218	7.702	8.323	8.841	9.36	9.83
25	2025/0 8/04	-61.69628	56.541676	138.5	118.5	98.5	78.5	58.5	38.5	5.439	5.853	6.541	6.941	7.533	8.129
26	2025/0 8/04	-61.70807904	56.54137606	134	114	94	74	54	34	4.489	5.514	6.08	6.677	7.987	8.667
27	2025/0 8/04	-61.70271912	56.5384509	144	124	104	84	64	44	4.126	4.624	5.288	5.628	6.034	7.558
28	2025/0 8/04	-61.71447077	56.53989563	145.5	125.5	105.5	85.5	65.5	45.5	3.513	3.66	3.963	4.296	5.091	5.823
29	2025/0 8/05	-61.68921375	56.54748867	90.5	70.5	50.5	30.5	10.5	-9.5	0.182	0.014	3.442	6.503	16.18	19.78
30	2025/0 8/05	-61.69473591	56.54657455	135.5	125.5	115.5	105.5	95.5	85.5	1.31	1.737	3.157	4.204	5.487	9.751
31	2025/0 8/05	-61.69685986	56.54487792	125.5	105.5	85.5	65.5	45.5	25.5	3.124	5.202	6.789	6.446	8.425	11.16
32	2025/0 8/05	-61.70097652	56.54603791	146	126	106	86	66	46	7.1	9.204	10.16	10.6	11.75	12.05

33	2025/0 8/05	-61.70514367	56.54463766	109.5	89.5	69.5	49.5	29.5	9.5	2.694	3.559	4.225	5.471	10.68	16.55
34	2025/0 8/05	61.700766	56.543552	143.3	123.3	103.3	83.3	63.3	43.3	2.354	2.999	3.933	4.518	5.154	6.592
35	2025/0 8/06	-61.69046493	56.53625249	137.3	117.3	97.3	77.3	57.3	37.3	12.6	12.87	13.7	14.29	18.37	20.91
36	2025/0 8/06	-61.69228988	56.53583643	137.5	117.5	97.5	77.5	57.5	37.5	2.671	4.4	6.05	6.65	7.919	8.999
37	2025/0 8/06	-61.69065415	56.53501976	138.8	118.8	98.8	78.8	58.8	38.8	3.22	4.535	5.32	6.375	7.146	7.382
38	2025/0 8/06	-61.68930063	56.5356137	143.2	123.2	103.2	83.2	63.2	43.2	0.89	2.052	2.721	3.01	4.183	5.27
39	2025/0 8/07	-61.69691615	56.54043778	140.3	120.3	100.3	80.3	60.3	40.3	6.404	6.802	7.611	8.071	9.196	10.71
40	2025/0 8/07	-61.69291479	56.53987939	149.4	129.4	109.4	89.4	69.4	49.4	7.866	8.27	8.909	9.322	10.01	11.32
41	2025/0 8/07	-61.69287283	56.54113478	89.2	69.2	49.2	29.2	9.2	-10.8	0.042	1.413	3.386	5.503	9.588	23.42
42	2025/0 8/07	-61.69300688	56.5420648	134.1	114.1	94.1	74.1	54.1	34.1	4.072	4.998	6.016	6.723	7.963	10.25
43	2025/0 8/07	-61.69479631	56.54144028	120.4	100.4	80.4	60.4	40.4	20.4	6.917	8.09	9.871	9.694	11	15.96
44	2025/0 8/07	-61.69682379	56.54081195	111.9	91.9	71.9	51.9	31.9	11.9	9.246	10.1	11.06	12	14.05	26.57
45	2025/0 8/07	-61.69002011	56.53244772	142.5	122.5	102.5	82.5	62.5	42.5	7.432	8.932	9.88	9.999	11.25	13.3
46	2025/0 8/07	-61.69079681	56.53053945	141.5	121.5	101.5	81.5	61.5	41.5	4.455	5.601	7.462	7.251	8.36	10.55
47	2025/0 8/07	-61.68823305	56.53035985	148.3	128.3	108.3	88.3	68.3	48.3	4.144	5.772	7.111	7.553	8.126	9.802
48	2025/0 8/07	61.708151	56.53674	140.5	120.5	100.5	80.5	60.5	40.5	6.465	6.919	7.506	8.132	8.305	10.4
49	2025/0 8/07	-61.707023	56.536781	140.7	120.7	100.7	80.7	60.7	40.7	4.04	4.478	5.218	5.908	6.95	8.546

50	2025/0 8/07	61.705184	56.537318	143.5	123.5	103.5	83.5	63.5	43.5	2.576	2.532	3.021	3.505	4.123	6.129
51	2025/0 8/08	-61.69131065	56.53994329	141.5	121.5	101.5	81.5	61.5	41.5	4.089	4.952	6.099	7.489	8.407	9.736
52	2025/0 8/08	-61.69077232	56.54023922	125.3	105.3	85.3	65.3	45.3	25.3	7.649	9.141	10.52	12.04	14.82	16.22
53	2025/0 8/08	-61.69031574	56.5404799	115.4	95.4	75.4	55.4	35.4	15.4	7.445	8.462	9.88	12.08	14.04	15.82
54	2025/0 8/08	-61.69173264	56.53975246	130.4	110.4	90.4	70.4	50.4	30.4	3.623	4.258	4.734	5.209	6.086	6.938
55	2025/0 8/08	-61.69174254	56.53988298	124.1	104.1	84.1	64.1	44.1	24.1	4.775	5.371	6.32	7.245	8.762	12.27
56	2025/0 8/08	-61.68931254	56.53987945	121.5	101.5	81.5	61.5	41.5	21.5	9.659	10.64	12.3	13.94	15.72	17.07
57	2025/0 8/08	-61.68915893	56.53997649	122.8	102.8	82.8	62.8	42.8	22.8	7.644	8.431	10	11.81	13.88	15.38
58	2025/0 8/08	-61.6894578	56.53978995	119.9	99.9	79.9	59.9	39.9	19.9	9.362	10.54	11.76	13.03	14.5	16.79
59	2025/0 8/08	-61.71840929	56.5364162	136	116	96	76	56	36	3.638	3.692	4.235	4.724	5.383	6.293
60	2025/0 8/08	-61.71885352	56.53681039	138.1	118.1	98.1	78.1	58.1	38.1	4.441	5.657	6.717	7.291	8.197	10.51
61	2025/0 8/08	-61.71912567	56.53706789	134.5	114.3	94.1	73.9	53.7	33.5	1.848	2.885	3.596	4.136	5.075	6.588
62	2025/0 8/10	-61.71917869	56.53720879	122.1	102.1	82.1	62.1	42.1	22.1	4.319	4.752	5.5	6.104	7.27	8.684
63	2025/0 8/10	-61.71910465	56.53747576	147.2	127.2	107.2	87.2	67.2	47.2	5.796	6.347	7.155	7.736	8.67	6.939
64	2025/0 8/10	-61.71920791	56.53770454	111.2	91.2	71.2	51.2	31.2	11.2	7.721	8.013	8.709	9.346	10.81	11.95
65	2025/0 8/10	-61.71945266	56.53809259	102.2	82.2	62.2	42.2	22.2	2.2	6.723	7.37	8.224	9.53	10.69	21.91
66	2025/0 8/10	-61.71947765	56.53821965	105.3	85.3	65.3	45.3	25.3	5.3	5.642	5.868	6.493	7.154	10.545	16.87

67	2025/0 8/10	-61.71808398	56.53798505	135.1	115.1	95.1	75.1	55.1	35.1	4.914	5.565	6.489	7.387	8.599	20.34
68	2025/0 8/10	-61.73079441	56.53757626	123.5	103.5	83.5	63.5	43.5	23.5	5.957	6.4	7.273	8.428	10.44	13.35
69	2025/0 8/11	-61.69437838	56.54619752	111.6	91.6	71.6	51.6	31.6	11.6	1.984	2.522	3.1514	3.973	5.519	8.255
70	2025/0 8/11	-61.69421284	56.54622723	126.3	106.3	86.3	66.3	46.3	26.3	1.691	2.507	3.607	4.478	6.418	9.13
71	2025/0 8/11	-61.69362475	56.54563744	106.9	86.9	66.9	46.9	26.9	6.9	2.815	3.614	4.439	5.577	7.226	9.837
72	2025/0 8/11	-61.6946464	56.54474609	106.8	86.8	66.8	46.8	26.8	6.8	4.621	5.698	6.892	8.314	10.43	12.01
73	2025/0 8/11	-61.69150882	56.54401263	103.6	83.6	63.6	43.6	23.6	3.6	5.577	6.857	8.656	10.35	11.23	12.5
74	2025/0 8/11	-61.69191811	56.54435871	118.5	98.5	78.5	58.5	38.5	18.5	7.857	8.233	8.726	9.369	11.27	12.75
75	2025/0 8/11	-61.69223259	56.54472283	125	105	85	65	45	25	4.126	4.684	5.517	5.489	7.595	9.331
76	2025/0 8/11	-61.69232706	56.5449887	119.5	99.5	79.5	59.5	39.5	19.5	2.967	3.172	3.733	4.59	5.676	8.266
77	2025/0 8/11	-61.7010802	56.53744758	132.4	112.4	92.4	72.4	52.4	32.4	2.327	2.409	2.988	3.827	4.587	5.521
78	2025/0 8/11	-61.70351791	56.53732224	144.1	124.1	104.1	84.1	64.1	44.1	2.923	3.342	3.791	4.257	5.111	6.085
79	2025/0 8/11	-61.70316068	56.53744011	143.5	123.5	103.5	83.5	63.5	43.5	5.737	6.236	7.075	7.721	8.671	9.391
80	2025/0 8/11	-61.69044173	56.54824411	104.2	84.2	64.2	44.2	24.2	4.2	2.512	3.487	4.999	6.843	9.124	11.05
81	2025/0 8/12	-61.69977308	56.53941485	120.3	100.3	80.3	60.3	40.3	20.3	5.738	6.766	8.038	9.544	10.13	11.1
82	2025/0 8/12	-61.71075203	56.53799578	118.5	98.5	78.5	58.5	38.5	18.5	9.817	10.46	11.27	11.97	12.45	12.85
83	2025/0 8/12	-61.70778209	56.54118071	147.2	127.2	107.2	87.2	67.2	47.2	1.949	2.542	3.013	4.389	9.351	12.583

84	2025/0 8/12	-61.69823639	56.53874515	145	125	105	85	65	45	3.571	4.556	4.894	5.429	6.239	7.445
----	----------------	--------------	-------------	-----	-----	-----	----	----	----	-------	-------	-------	-------	-------	-------

**Table A6:** All CAS temperature points

## Appendix A7

CAS #	Method	Organic Layer Thickness	Max Vegetation Height	Percent Cover of Vegetation	Disturbed?	Fill	Canopy Cover	Soil Moisture	Soil Texture	Surficial Material	Vegetation	Snow Cover	Drainage Class	Slope
1	Both		99	100	no	no	0	Hydric		Organic	Herbaceous	protected	Poor	middle slope
2	Both		13	100	no	no	0	Mesic	Sand	Marine, Organic	Moss, Herbaceous	neutral	Moderate	middle slope
3	Both		160	100	no	no	0	Mesic	Loam	Marine	High Shrub, Herbaceous	very protected	Moderate	middle slope
4	Both	14	93	100	no	no	0	Hygic	Loamy Sand	Marine	Herbaceous	protected	Poor	middle slope
5	Both	19	33	100	no	no	0	Hygic	Loamy Sand	Marine	Moss, Low Shrub, Herbaceous	neutral	Moderate	middle slope
6	Frost Probe	4	16	100	no	no	0	Mesic	Sandy Loam	Marine	Prostrate Shrub	protected	Moderate	middle slope
7	Both	0	27	10	yes	no	0	Xeric	Sand	Marine	Low Shrub	exposed	Rapid	lower slope
8	Frost Probe	10	250	100	no	no	0	Hydric	Sandy Clay Loam	Organic	High Shrub, Herbaceous	very protected	Poor	toe
9	Frost Probe	16	250	100	no	no	90	Hydric	Clay	Organic	High Shrub, Herbaceous	very protected	Poor	lower slope
10	Frost Probe	10	45	95	yes	no	0	Hydric	Loamy Sand	Marine	Herbaceous	exposed	Poor	toe
11	Hand drill	27.5	68	100	no	no	0	Mesic	Loamy Sand	Glacial, Colluvial	Low Shrub	protected	Moderate	lower slope
12	Both	29	30	70	no	no	0	Mesic	Loamy Sand	Glacial	Prostrate Shrub	exposed	Moderate	middle slope
13	Hand drill	11	23	85	no	no	0	Hygic	Loamy Sand	Glacial	Prostrate Shrub	exposed	Moderate	middle slope
14	Hand drill	35	102	100	no	no	90	Mesic	Loamy Sand	Glacial	High Shrub, Herbaceous	very protected	Moderate	upper slope,



28	Frost Probe	20	600	100	no	no	25	Mesic	Loam	Organic, Glacial, Colluvial	Tree (Coniferous), Moss, Prostrate Shrub	protected	Poor	level
29	Both	13	40	100	no	no	0	Mesic	Loamy Sand	Glacial, Colluvial	Low Shrub	neutral	Moderate	lower slope
30	Frost Probe	14	52	100	no	no	0	Xeric	Sand	Glacial, Colluvial	Low Shrub, Prostrate Shrub, Lichen	protected	Moderate	middle slope
31	Both	20	60	100	no	no	10	Mesic	Loamy Sand	Glacial, Colluvial	Moss, Low Shrub, Tree (deciduous)	very protected	Moderate	middle slope
32	Frost Probe	8.5	34	90	no	no	0	Xeric	Sand	Glacial	Prostrate Shrub, Low Shrub	exposed	Rapid	upper slope
33	Both	15	100	100	no	no	10	Mesic	Sandy Loam	Bedrock Till	Prostrate Shrub, Moss, Low Shrub, Tree (Coniferous)	protected	Moderate	upper slope
34	Frost Probe	15	64	100	no	no	20	Mesic	Loamy Sand	Glacial, Colluvial	Prostrate Shrub, Low Shrub, Moss, Tree (Coniferous)	very protected	Rapid	level
35	Both	0	8	1	yes	no	0	Xeric	Sand	Disturbed		very exposed	Rapid	lower slope
36	Frost Probe	0	66	100	yes	no	0	Mesic	Sand	Disturbed	Moss, Low Shrub, Tree (Coniferous), Herbaceous	exposed	Rapid	middle slope
37	Frost Probe	11	42	70	yes	no	0	Xeric	Sand	Disturbed	Lichen, Low Shrub, Prostrate Shrub	exposed	Rapid	middle slope

38	Frost Probe	6	65	100	yes	no	0	Mesic	Sand	Disturbed	Low Shrub, Prostrate Shrub	protected	Rapid	middle slope
39	Frost Probe	8	300	50	yes	no	100	Xeric	Sand	Marine	High Shrub, Herbaceous	very protected	Rapid	lower slope
40	Frost Probe	0	100	20	yes	no	100	Mesic	Sand	Marine	Moss, High Shrub, Herbaceous	very protected	Moderate	crest
41	Both	13	30	100	no	no	0	Hygric	Loamy Sand	Marine	Low Shrub, Herbaceous	exposed	Poor	middle slope
42	Frost Probe	0	45	10	yes	no	50	Mesic	Sand	Marine	Tree (Coniferous), Herbaceous	exposed	Rapid	upper slope
43	Frost Probe	7	200	10	yes	yes	10	Xeric	Sand	Fluvial	High Shrub, Herbaceous	neutral	Rapid	middle slope
44	Both	0	140	30	yes	yes	0	Xeric	Clay Sand	Marine	High Shrub, Herbaceous	exposed	Rapid	upper slope
45	Frost Probe	0	44.5	50	yes	no	0	Mesic	Sand	(the quarry)	Low Shrub, Herbaceous	very exposed	Rapid	middle slope
46	Frost Probe	22	43	100	no	no	3	Mesic		(the quarry)	Low Shrub, Prostrate Shrub, Tree (Coniferous)	protected	Moderate	middle slope
47	Frost Probe	21	65	100	no	no	0	Xeric	Loamy Sand	(the quarry)	Moss, Low Shrub, Prostrate Shrub, Tree (Coniferous)	protected	Moderate	level
48	Frost Probe	5	320	50	no	no	20	Hygric	Loamy Sand	Alluvial	High Shrub, Herbaceous	very protected	Moderate	level
49	Frost Probe	9	200	100	no	no	0	Hygric	Sand	Alluvial	Low Shrub, High Shrub, Herbaceous	very protected	Poor	level

50	Frost Probe	15	13.8	100	no	no	70	Hygic	Clay	Alluvial	Moss, Low Shrub, Tree (Coniferous)	protected	Poor	level
51	Frost Probe	4	115.5	100	yes	no	100	Xeric	Sand	Marine	Low Shrub, Herbaceous	protected	Moderate	upper slope
52	Frost Probe	0	0	0	yes	yes	0	Mesic	Sand	Fill		very exposed	Rapid	level
53	Both	0	0	0	yes	yes	0	Mesic	Sand	Fill		very exposed	Rapid	level
54	Frost Probe	3	200	100	no	no	0	Hydric	Clay Sand	Marine	Herbaceous, Low Shrub, Moss	protected	Poor	level
55	Frost Probe	6	187	100	no	no	0	Mesic	Loamy Sand	Marine	Low Shrub, High Shrub, Herbaceous	protected	Moderate	crest
56	Frost Probe	0	35	5	yes	yes	0	Xeric	Sand	Fill	Herbaceous	very exposed	Rapid	level
57	Frost Probe	0	51	40	yes	yes	0	Xeric	Sand	Fill	Herbaceous	very exposed	Rapid	level
58	Frost Probe	0	52	20	yes	yes	0	Xeric	Sand	Fill	Herbaceous	very exposed	Rapid	level
59	Frost Probe	13	59	100	no	no	10	Hygic	Clay loam	Glacial, Colluvial	Moss, Tree (Coniferous), Prostrate Shrub	protected	Poor	middle slope
60	Both	9	49	100	no	no	0	Mesic	Loamy Sand	Glacial, Colluvial	Moss, Prostrate Shrub, Low Shrub	neutral	Moderate	middle slope
61	Frost Probe	9	61	100	no	no	20	Mesic	Sandy Loam	Glacial, Colluvial	Moss, Prostrate Shrub, Low Shrub, Tree (Coniferous)	protected	Moderate	middle slope
62	Frost Probe	23	57.6	100	no	no	0	Mesic	Sandy Loam	Glacial, Colluvial	Prostrate Shrub, Low Shrub	protected	Moderate	middle slope

63	Frost Probe	15	66	100	no	no	50	Hygric	Loamy Sand	Glacial, Colluvial	Prostrate Shrub, Low Shrub, Moss, Tree (Coniferous)	protected	Moderate	middle slope
64	Both	8	66	100	no	no	0	Hygric	Sandy Loam	Glacial, Colluvial	Low Shrub, Prostrate Shrub	neutral	Poor	middle slope
65	Drill	16	72	100	no	no	0	Hydric	Loamy Sand	Glacial, Colluvial	Prostrate Shrub, Low Shrub, Moss	neutral	Poor	middle slope
66	Frost Probe	31	65	100	no	no	50	Hygric	Loamy Sand	Glacial, Colluvial	Moss, Low Shrub, Prostrate Shrub, Tree (Coniferous)	protected	Poor	middle slope
67	Frost Probe	13	28	100	no	no	20	Mesic	Sand	Glacial, Colluvial	Moss, Low Shrub, Tree (Coniferous)	protected	Rapid	middle slope
68	Frost Probe	>30	31	100	no	no	0	Hydric	Organic	Organic	Herbaceous	exposed	Poor	level
69	Frost Probe	22	100	100	no	no	0	Mesic	Loamy Sand	Glacial, Colluvial	Moss, Prostrate Shrub, Low Shrub, Tree (Coniferous)	protected	Rapid	middle slope
70	Drill	10	70	100	no	no	30	Mesic	Loamy Sand	Glacial, Colluvial	Low Shrub, Prostrate Shrub, Moss, Tree (Coniferous)	protected	Moderate	middle slope
71	Both	17	75	100	no	no	0	Hygric	Sandy Loam	Glacial, Colluvial	Moss, Low Shrub, Prostrate Shrub, Tree (Coniferous)	protected	Poor	middle slope

72	Both	18	58	100	no	no	50	Hygric	Sand	Glacial, Colluvial	Moss, Low Shrub, Prostrate Shrub, Tree (Coniferous)	protected	Moderate	lower slope
73	Frost Probe	7	125	100	yes	yes	0	Hygric	Sand	Fill	Herbaceous, Low Shrub	neutral	Rapid	level
74	Drill	>30	160	100	yes	yes	10	Hygric	Loamy Sand	Fill	Herbaceous, High Shrub	neutral	Moderate	lower slope
75	Both	13	200	100	no	no	10	Hygric	Loamy Sand	Colluvial, Glacial	Moss, Low Shrub, Prostrate Shrub, High Shrub	protected	Moderate	toe
76	Both	17	130	100	yes	no	0	Hygric	Sand	Glacial, Colluvial	Herbaceous, Tree (Coniferous), High Shrub	neutral	Moderate	lower slope
77	Frost Probe	>30	105	100	no	no	0	Hydric	Organic	Alluvial	Moss, Low Shrub, Tree (Coniferous)	protected	Poor	level
78	Frost Probe	17	81	100	no	no	70	Hydric	Sand	Alluvial	Herbaceous, Low Shrub, Tree (Coniferous), Prostrate Shrub	protected	Poor	level
79	Frost Probe	15	73	100	no	no	10	Hydric	Sandy Loam	Alluvial	Low Shrub, Herbaceous	protected	Poor	level
80	Frost Probe	19	20	50	no	no	0	Mesic	Sand	Glacial, Colluvial	Lichen, Low Shrub, Herbaceous	exposed	Rapid	middle slope
81	Frost Probe	7	98	40	yes	no	0	Hygric	Sand	Glacial, Fluvial	Herbaceous, Low Shrub	protected	Rapid	middle slope
82	Frost Probe	0	83	20	yes	yes	0	Hygric	Loamy Sand	Disturbed	Low Shrub, Herbaceous	exposed	Poor	upper slope

83	Frost Probe	>30	73	100	no	no	60	Mesic	Organic	Glacial, Fluvial	Prostrate Shrub, Low Shrub, Tree (Coniferous)	protected	Moderate	crest
84	Frost Probe	7	54	100	yes	no	100	Hygic	Organic	Glacial, Fluvial	Moss, Low Shrub, Tree (Coniferous)	very protected	Moderate	upper slope

**Table A7:** All CAS variables.